Florida State University Libraries

2011

Lightning Observations during Tropical Cyclone Intensity Change: A Composite Study of Spatial and Temporal Relationships

Marcus Austin

THE FLORIDA STATE UNIVERSITY

COLLEGE OF ARTS AND SCIENCES

LIGHTNING OBSERVATIONS DURING TROPICAL CYCLONE INTENSITY CHANGE: A

COMPOSITE STUDY OF SPATIAL AND TEMPORAL RELATIONSHIPS

By

MARCUS AUSTIN

A Thesis submitted to the
Department of Earth, Ocean and Atmospheric Science
in partial fulfillment of the
requirements for the degree of
Master of Science

Degree Awarded:
Spring Semester, 2011

The members of the committee approve the thesis of Marcus Austin defended on November 4, 2010.

_____
Henry Fuelberg
Professor Directing thesis

_____
Robert Hart
Committee Member

_____
Paul Ruscher
Committee Member

The Graduate School has verified and approved the above-named committee members.

I dedicate this work firstly to my family who supported me and provided constant encouragement along the way. I also dedicate this thesis to my wife of two years who not only motivated me, but pushed me to pursue my love of meteorology and science and sacrificed much for my endeavors.

ACKNOWLEDGEMENTS

I must first thank my parents, Danny and Eva Austin who facilitated my appreciation for learning from an early age. Over the years they have provided endless encouragement, love and monetary support so that I may obtain this advanced degree. They have worked tirelessly and without complaint to see me succeed and I will forever appreciate their sacrifices. I also thank my siblings, John, Paul, and Sarah, who have been an integral part of my life. They have shaped my life and my future in ways they cannot imagine and I am forever grateful to them. With two wonderful years of marriage, my wife remains of utmost importance in my life. She has always encouraged me and pushed me when things seemed unreachable and she has put up with me for the duration of this scholarly work. I love and thank her for all that she is and all she offers me every day. She truly is the love of my life, and without her, this accomplishment would not have been possible.

I thank my friends and lab mates who were always there to cheer me up and provide feedback when I was unsure of my results. I thank them for providing some comic relief during those stressful times when things weren't going as planned and I needed a good laugh, and for the times when I just needed to chat.

Finally I thank all of my professors who provided me a solid background on which to build my scientific knowledge. I thank them for taking the time to teach me all that I have learned and all that has become part of my educational career. I thank them for having an open door and an open mind when I was confused or needed feedback on my scientific method and results. These professors are truly some of the best in the country and I could not have succeeded without any of them.

Finally, I thank my major professor, Dr. Henry Fuelberg, who informally goes by HEF and has more patience and heart than anyone I have encountered. He has given moral support and encouragement through this endeavor and has believed in me even when I did not. He is a true mentor and friend for whom I have great respect.

TABLE OF CONTENTS

LIST OF TABLES

LIST OF FIGURES

ABSTRACT

Although tropical cyclone (TC) track forecasts have improved considerably in recent years, predicting their intensity continues to be a challenge for both meteorologists and numerical models. A storm's path is primarily influenced greatly by large-scale atmospheric circulations; however, its strength appears to be dominated both by large scale influences and small-scale mechanisms within the storm itself. Most previous research on TC intensity change has employed either numerical modeling or diagnostic approaches using traditional meteorological parameters. Only recently have studies begun to examine electrification as a means for assessing the potential for intensification. Several papers have considered lightning as a proxy for storm intensification, mostly using data from Vaisala's National Lightning Detection Network (NLDN) and Long-Range Lightning Detection Network (LLDN). However, they mostly have examined individual TCs.

This study uses LLDN data to study 45 Atlantic Basin TCs between the years 2004 and 2008. Using the National Hurricane Center's (NHC) best track dataset, lightning data are collected for each TC out to a 500 km radius. Parameters including storm intensity, intensity change, environmental vertical wind shear, storm motion, and flash count are compiled at each NHC best track position. The data at each position then are categorized in several ways, including change in intensity. These methods allow us to examine relations between composites of storm intensity/intensification and convective distribution and frequency.

Distributions of cloud-to-ground (CG) flash density with respect to storm motion and speed show that lightning generally is preferred in the TCs' right front and right rear quadrants. Hurricanes produce the greatest flash densities during relatively slow forward motion, while tropical depressions and tropical storms exhibit greater flash densities during faster forward motion. Storm-relative CG flash distributions during weakening, no pressure change, and slow intensification (-5 to 0 hPa 6 h^{-1}) exhibit the same right front and rear quadrant preference as the TC intensity categories. Flash densities are greatest during periods of faster intensification, with a nearly symmetric presentation in the inner core region.

When computing flash densities with respect to environmental deep layer wind shear, TCs exhibit a strong preference for lightning in the downshear left and right quadrants of the inner

core (0-100 km) and outer rainbands (100-300 km), respectively. Tropical storms and hurricanes best show this relation, with TDs exhibiting a stronger preference for lightning in the downshear right quadrant. Relatively weak wind shear produces greater flash densities in all TC intensity categories. Conversely, storms experiencing strong shear exhibit smaller flash densities in all TC categories due to the disruption of deep convection. During periods of faster intensification, maximum flash densities are located in the inner core, with weakening, no change, and slow intensification periods containing greatest density in the outer rainbands. Average flash rates and flash densities are found to be greatest for weaker TCs (tropical depressions and tropical storms) with smaller flash rates and densities in hurricanes.

Considering intensity change, periods of faster intensification exhibit significantly greater flash rates than periods of weakening, no pressure change, and slow intensification. Only weak relations are found between flash rates and intensity change, with the strongest relationship occurring when lightning lags (occurs after) the pressure change period. Lightning preceding (occurring before) the pressure change period exhibits the weakest relationships in all TC intensities. Correlations between CG lightning and sustained wind speed indicate that there is no preferred timing between maximum lightning activity and maximum sustained winds. Instead, maximum correlations occur during periods when greatest lightning activity both precedes and lags the maximum sustained wind. These results indicate that lightning is poorly correlated with intensity change and can be regarded as a poor choice for intensity forecasting.

CHAPTER 1

INTRODUCTION

Our understanding of tropical cyclones (TCs) has improved greatly in recent decades. The increasing availability of buoy and satellite data as well as aircraft reconnaissance observations have contributed to more accurate TC track forecasts (Fig. 1a) (e.g., Goerss et al. 2004; Aberson 2002, 2003, 2010); however, TC intensity forecasting continues to perplex the scientific community. There has been virtually no improvement in TC intensity forecasts during recent decades (Fig. 1b) (e.g., DeMaria and Kaplan 1999; DeMaria et al. 2005; Krishnamurti et al. 2005; Houze et al. 2006).
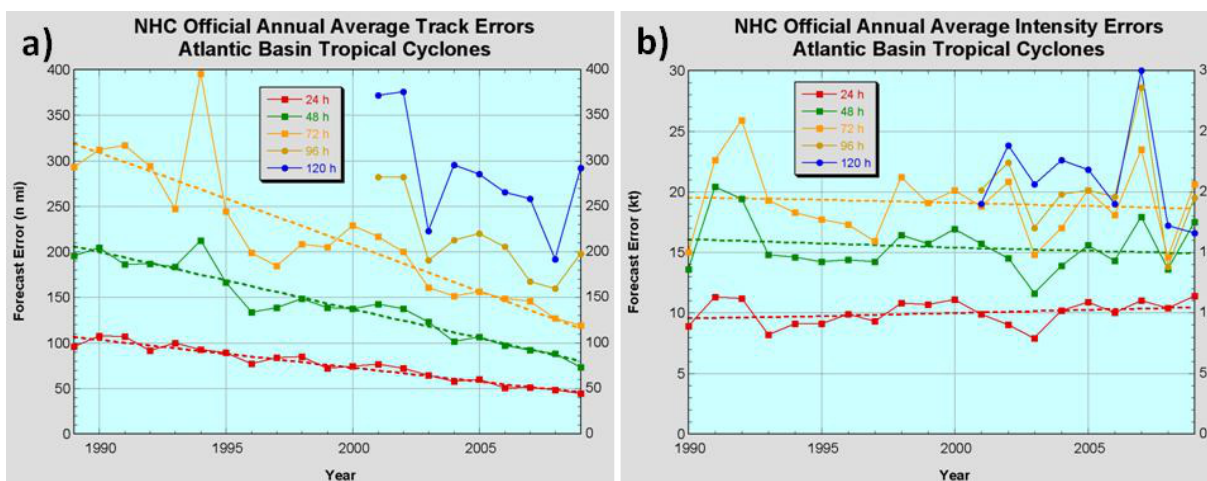
Figure 1. National Hurricane Center (NHC) a) annual average track errors (1990-2009) and b) annual average intensity errors (1990-2009) (from NHC's forecast verification page http://www.nhc.noaa.gov/verification/verify5.shtml?).

Tropical cyclones primarily have been monitored using infrared and visible satellite imagery from geostationary platforms, microwave imagery from polar-orbiting satellites, and aircraft reconnaissance. Of these, only geostationary satellite data provide nearly continuous surveillance of tropical features; however, these data often are degraded by TC-related cirrus that can mask

important structural features. Polar-orbiting satellites make infrequent passes over individual features, and aircraft data are only available intermittently.

Lightning has been investigated as a possible indicator of TC intensification. Lightning observations over oceanic regions have increased with the development of several detection networks including the World Wide Lightning Location Network (WWLLN) (Jacobson et al. 2006, Rodger et al. 2005, 2006), Vaisala's National Lightning Detection Network (NLDN), Long Range Lightning Detection Network (LLDN), and most recently, the Global Lightning Dataset (GLD360) (Demetriades and Holle 2005, 2008; Demetriades et al. 2006, 2010). Data from these networks are useful in monitoring TCs since they provide real-time continuous information during both day and night, can monitor TC convection over the open oceans, and in the case of the WWLLN and GLD360, globally. The development of these networks has enabled forecasters and scientists to observe convectively active regions within TCs.

Investigations of lightning in the tropics are not new. Studies have emphasized the relevance of lightning frequency and distribution as possible signals of TC intensity change (Lyons and Keen 1994; Samsury and Orville 1994; Molinari et al. 1994, 1999; Corbosiero and Molinari 2002, 2003; Demetriades et al. 2006, 2010; Squires and Businger 2008; Demetriades and Holle 2005, 2008; Price et al. 2009; Abarca et al. 2010; Molinari and Vollaro 2010). Recent research also has focused on electrical activity in tropical waves (Leppert II and Petersen 2010; Leary and Ritchie 2009). Each has attempted to provide new understanding about the role of lightning in TCs, and more importantly, whether lightning data can be used to improve both short and long-term intensity forecasts.

The role of microphysical properties that lead to lightning generation within TCs and tropical convection has received considerable attention (Black and Hallet 1986, 1999; Cecil and Zipser 1999; Cecil et al. 2002a, b; Toracinta et al. 2001, 2002; Fierro et al. 2007; Khain et al. 2008, 2010). Wiloughby et al. (1985) and Black and Hallett (1986, 1999) were among the first to study the role of cloud microphysics in the electrification of TCs. They found that outside of strong convective cells in the inner core and outer rainbands, TCs lacked sufficient supercooled water to produce large amounts of lightning. Lightning was most common in updrafts exceeding 5 m s^{-1} because they contained more supercooled droplets, graupel, and ice particles above the melting level. Furthermore, updraft speeds and lightning associated with typical oceanic convection and tropical systems have been found to be much less than those of typical mid-

latitude continental thunderstorms (Zipser and LeMone 1980; Jorgensen 1984; Willis and Marks 1987; Jorgensen and LeMone 1989; Lucas et al. 1994; Igau et al. 1999).

Passive microwave techniques have been employed to study the lightning and microphysics in TCs. Cecil and Zipser (1999), Cecil et al. (2002a, b) and Toracinta et al. (2002) used the Tropical Rainfall Measuring Mission (TRMM) satellite to observe 85 GHz and 37 GHz brightness temperatures as well as associated total (intra-cloud (IC) plus cloud-to-ground (CG)) lightning from the TRMM Lightning Imaging Sensor (LIS). They determined that lightning frequency was greater for tropical continental convection than for tropical oceanic systems because the continental storms contained stronger updrafts that could support larger quantities of ice particles and graupel above the melting level. Cecil et al. (2002a, b) analyzed characteristics of lightning and ice scattering by categorizing storms into three radial regions. Their results indicated that lightning was most prevalent in the regions farthest from the storm center (the outer rainbands), with somewhat less activity in the eyewall and a minimum in the inner rainbands. Fierro et al. (2007) simulated a hurricane-like vortex, with results showing maximum total lightning in the eyewall and outer rainband regions where the strongest updrafts were located.

The role of aerosols in relation to TC lightning also has been explored (e.g., Khain et al. 2008, Sun et al. 2008; Khain et al. 2010). Khain et al. (2008) focused on the role of landfall in the lightning pattern and whether continental aerosol intrusion was important in cloud electrification. Using a 2D mixed-phase cloud model, they found that the introduction of aerosols into TCs increased the content of ice and supercooled water and updraft strength in outer rainband convection, leading to greater lightning activity. Similarly, Khain et al. (2010) used the WRF model and spectral bin microphysics to simulate the impact of aerosols on hurricane Katrina (2005). Their results showed that aerosol entrainment ~20 h before Katrina (2005) made landfall resulted in weakening and increased lightning at the TC's periphery. These studies argued that landfalling TCs would experience an increase in outer rainband lightning, inner-core flash rates would decrease as the TC weakened, and that increased eyewall lightning was due to eyewall replacement.

Regarding the distribution of lightning in TCs, Samsury and Orville (1994) described cloud-to-ground (CG) lightning in Hurricanes Hugo (1989) and Jerry (1989). Their results and those of others (Lyons et al. 1989; Lascody 1993; Lyons and Keen 1994; Molinari et al. 1999) indicated

that lightning activity was most common in the outer rainbands. Molinari et al. (1999) went farther, saying that CG lightning could be used to define specific regions in TCs, finding flash maxima in the eyewall (~40-60 km), a distinct minimum in the inner rainbands (80-100 km), and peak lightning activity in the outer rainbands (~200-300 km). Relating lightning activity to storm speed and vertical wind shear has provided similar results regarding this radial distribution (Corbosiero and Molinari 2002, 2003; Molinari et al. 2004; Wingo and Cecil 2008; Molinari and Vollaro 2010). High reflectivity and enhanced CG lightning were most common in the downshear-left and downshear-right portions of the inner core and outer rainbands, respectively, with these quantities greatest to the right of storm motion.

Lyons and Keen (1994) argued for a relationship between rapid increases in inner core lightning (often called bursts or jumps) and TC intensification. Their study of Hurricanes Diana (1984) and Florence (1988) indicated that bursts preceded TC intensification. In a case study of Hurricane Andrew (1992), Molinari et al. (1994) also found that lightning bursts preceded deepening, and occurred during RI. Similarly, Squires and Businger (2008) assessed CG lightning in Hurricanes Katrina (2005) and Rita (2005) using Vaisala's LLDN. Their results suggested that eyewall lightning "outbreaks" were consistent with periods of rapid intensification (RI) and that peak flash activity occurred at maximum TC intensity (Demetriades and Holle 2005, 2008; Demetriades et al. 2006, 2010). Price et al. (2009) recently proposed that maximum lightning activity in intense mature hurricanes precedes maximum sustained wind speeds by approximately 24 h, and that above normal lightning activity over Eastern Africa may foretell more active Atlantic hurricane seasons. Conversely, other studies have shown that fluctuations in inner core lightning do not guarantee subsequent strengthening, but that lightning bursts also occur during periods of weakening or with little to no pressure change (Demetriades and Holle 2008; Demetriades et al. 2010).

Despite the considerable research about the relation between lightning and TCs, there is still much uncertainty about how lightning flash rates and their distributions relate to past, present, and future intensity, and more importantly, to intensity change. Although previous studies generally have found similar preferred lightning locations, especially in intense TCs, few studies have examined how these distributions vary with storm intensity. And, although numerous studies have considered the relation between inner core (IC) lightning and TC intensification, their often conflicting results have not produced consistent relationships.

Most of the studies cited above considered small numbers of TCs. However, we take a broader approach by examining 45 TCs of various intensities. LLDN lightning observations from these TCs are employed. Categorical lightning distributions with respect to shear and storm motion, and during different rates of intensity change, are presented to show whether there are consistent relationships between lightning activity and intensification. Finally, relationships between pressure change and flash rate in the inner core (0-100 km), outer rainbands (100-300 km), and far outer bands (300-500 km) are provided to determine whether there are any correlative relationships between region-specific lightning frequency and TC intensity and intensity change. By examining this extensive dataset, we seek to discover if there are general relationships between lightning and TCs.

The next section presents our research methodology, including data sources and computations. Section three provides detailed results and compares our findings with those of previous studies. Finally, section 4 presents concluding remarks that summarize our major findings.

CHAPTER 2

DATA AND METHODS

2.1 Lightning Detection

Several sources of lightning data were considered for use. The World Wide Lightning Location Network (WWLLN) currently consists of ~40 sensors and can monitor globally both in-cloud (IC) and cloud-to-ground (CG) lightning (Rodger et al. 2005, 2006; Jacobson et al. 2006; http://webflash.ess.washington.edu/). WWLLN's major limitation is its small detection efficiency (DE) (Rodger et al. 2006).

Vaisala's National Lightning Detection Network (NLDN) has been used in previous TC electrification studies and provides large DE (~80-90%) over North America (e.g., Orville and Silver 1997; Boccippio et al. 2000; Cummins et al. 1998; Idone et al. 1998a, b, Orville and Huffines 2001; Orville et al. 2002; Murphy and Holle 2005; Cummins et al. 2006; Orville 2008). However, its DE decreases rapidly from the U.S. coastline, making TC observations beyond a few hundred kilometers unreliable. The Global Lightning Dataset (GLD360), also supported by Vaisala, provides global lightning coverage with an average DE of 70% to 80% (Demetriades et al. 2010). However, since it only became operational during 2008, its data were not available for our entire study period.

Vaisala's Long Range Lightning Detection Network (LLDN) uses the NLDN, the Canadian Lightning Detection Network (CLDN), and sensors in the Pacific and Caribbean Basins to detect CG lightning farther from the coast than the NLDN (Demetriades and Holle 2005, 2008; Demetriades et al. 2006; Pessi et al. 2009; Demetriades et al. 2010). The LLDN provides improved DE farther from the coastline (Demetriades and Holle 2005, 2008; Demetriades et al. 2006, 2010; Squires and Businger 2008; Pessi et al. 2009; Abarca et al. 2010). Thus, the LLDN was selected for use in this study. LLDN daytime and nighttime DE is shown in Fig. 2. The LLDN uses time of arrival (TOA) and magnetic direction finding (MDF) technology to locate cloud-to-ground (CG) lightning at long distances by detecting lightning-induced ionospheric propagations called "sferics" (Pessi et al. 2009). Due to ionospheric variations between day and

night, the DE changes diurnally (Fig. 2), with greatest average DE at night and least detection during the daylight hours (Cramer and Cummins 1999; Demetriades and Holle 2005, 2008; Demetriades et al. 2006, 2010, Pessi et al. 2009).

LLDN stroke data were gathered for each storm selected for study and were compiled into flashes following the methods of Cummins et al. (1998). CG flashes were retained if they occurred within +/- 1.5 h of the National Hurricane Center's (NHC) interpolated 3 hourly best track center positions and were within 500 km of the storm center, similar to that of Demetriades and Holle (2008). As an example, for a TC position at 1200 UTC, flashes between 1030 and 1330 UTC would be assigned to 1200 UTC. This approach yielded a continuous field of CG lightning flashes out to a 500 km radius for each storm in the sample. We also examined 6 h periods, in which case flash data from +/- 3 h were assigned to the current observation.

Following Demetriades and Holle (2008), flash corrections were utilized to account for the diurnal and distance variations in DE. A set of DE grid points were used to obtain the estimated DE within 250 km of each TC center position. This produced a realistic estimate of the "actual" lightning activity occurring with each storm from its genesis to dissipation.
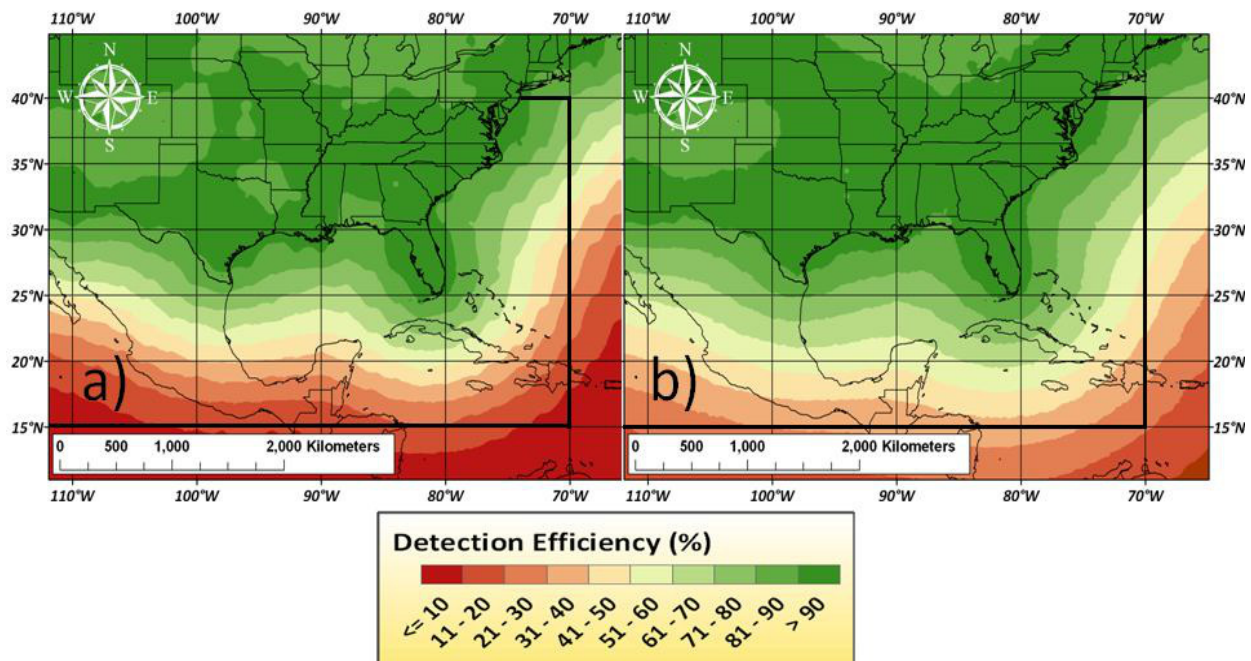
Figure 2. LLDN detection efficiency for a) daytime and b) nighttime within the study domain (thick black line) (After Demetriades and Holle 2008; Pessi et al. 2009)

2.2 Tropical Cyclone Sample and Domain

Since the DE of the LLDN generally decreases from the coastline (Fig. 2), our dataset was limited to TC locations that were approximately within the 40-50% nighttime DE contour (Fig. 2b). This corresponded to storms positioned north of 15º N latitude, south of 40º N latitude, and west of 70º W longitude. Although this restriction limited the number of observed periods per TC and omitted some storms completely, those locations that were used are in regions of reasonable Des to maintain data quality and limit location accuracy errors. Our dataset consisted of 45 Atlantic Basin TCs between 2004 and 2008 that satisfied the LLDN detection criteria described above. TCs prior to 2004 were not considered since the NLDN, part of the LLDN, was upgraded during 2002 and 2003 (Cummins and Murphy 2009). Fig. 3 shows the locations of all 6 h positions of the 45 TCs
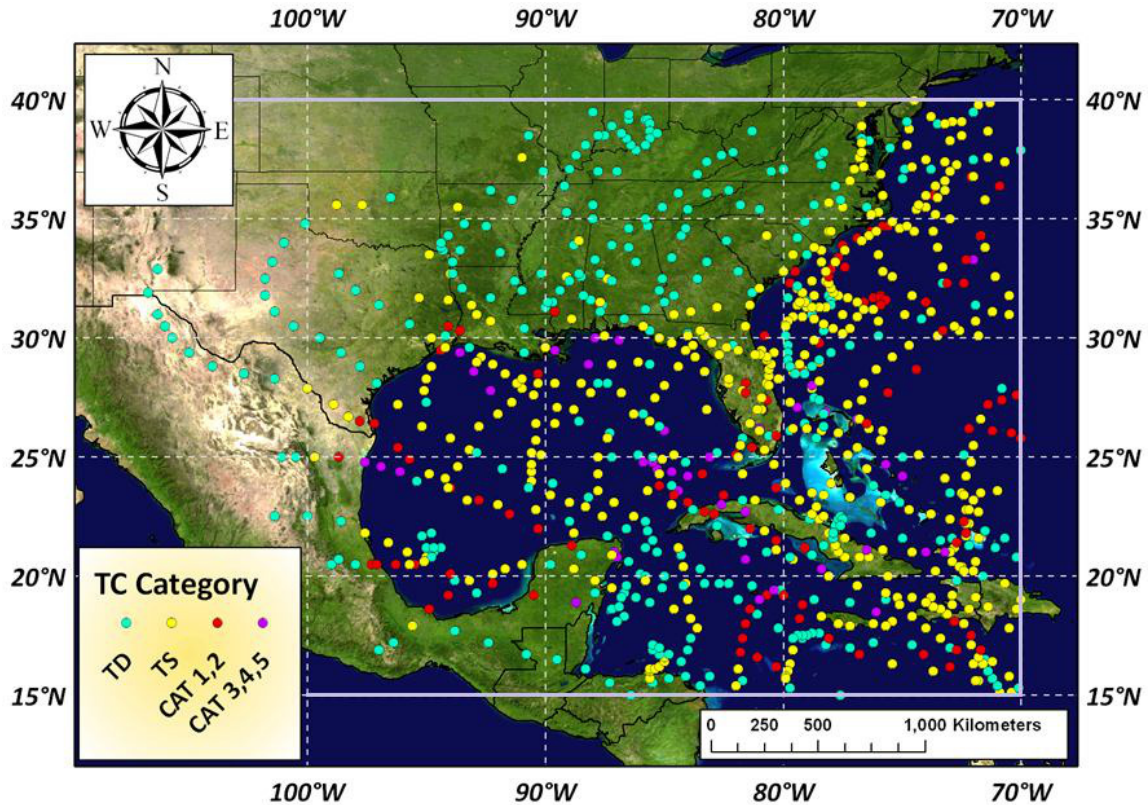
Figure 3. 6 h NHC best-track positions of the 45 storms within the study domain (thick gray line) during the 4 y study period. Storm locations had to be within the 40-50% nighttime DE contour (Fig. 1b). Each position is classified by intensity from TDs (turquoise) to Category 3+ hurricanes (purple).

within the domain. As in Corbosiero and Molinari (2002, 2003), 6 h positions over land were considered to be as valuable as those over water and thus were retained for flash density calculations, but were excluded from correlation computations due to the impact of land on regional flash frequency. The observation restrictions produced 1038 6 h and 2054 3 h positions for the combination of all TC intensities shown in Fig. 4. Table 1 lists the storms included, the years when they occurred, their number of 6 h periods, their minimum central pressures, maximum sustained winds, and peak intensities. This collection represents a wide variety of storms and is sufficiently large for this study. Fig. 4 shows the distribution of wind speeds (kt) for all 1038 6 h positions and thresholds for each TC intensity category.

Table 1. TCs comprising our dataset.

Storm Name (year)	Number of 6 h Periods (n)	Minimum Pressure (hPa)	Maximum Wind Speed (kt)	Maximum Intensity
Alex (2004)	16	957	105	Category 2
Bonnie (2004)	34	1001	55	Tropical Storm
Charley (2004)	18	941	130	Category 4
Frances (2004)	30	935	125	Category 4
Gaston (2004)	17	985	65	Category 1
Hermine (2004)	6	1002	50	Tropical Storm
Ivan (2004)	58	910	145	Category 5
Jeanne (2004)	40	950	105	Category 3
Matthew (2004)	12	997	40	Tropical Storm
Alpha (2005)	7	998	45	Tropical Storm
Arlene (2005)	18	989	60	Tropical Storm
Cindy (2005)	22	991	65	Category 1
Dennis (2005)	40	930	130	Category 4
Emily (2005)	22	929	140	Category 5
Franklin (2005)	15	997	50	Tropical Storm
Gamma (2005)	21	1002	45	Tropical Storm
Gert (2005)	9	1005	40	Tropical Storm
Katrina (2005)	30	902	150	Category 5
Ophelia (2005)	45	976	75	Category 1
Rita (2005)	33	895	155	Category 5
Stan (2005)	16	977	70	Category 1
Tammy (2005)	8	1001	45	Tropical Storm
Wilma (2005)	39	882	160	Category 5
Alberto (2006)	20	995	60	Tropical Storm
Beryl (2006)	11	1000	50	Tropical Storm

Table 1 - continued…

Storm Name (year)	Number of 6 h Periods (n)	Minimum Pressure (hPa)	Maximum Wind Speed (kt)	Maximum Intensity
Chris (2006)	10	1001	55	Tropical Storm
Ernesto (2006)	31	985	65	Category 1
Andrea (2007)	30	1001	65	Category 1
Barry (2007)	19	997	50	Tropical Storm
Dean (2007)	17	905	150	Category 5
Erin (2007)	20	1003	35	Tropical Storm
Felix (2007)	7	929	150	Category 5
Gabrielle (2007)	13	1004	50	Tropical Storm
Humberto (2007)	10	985	80	Category 1
Lorenzo (2007)	13	990	70	Category 1
Noel (2007)	29	980	70	Category 1
Olga (2007)	18	1003	50	Tropical Storm
Cristobal (2008)	13	998	55	Tropical Storm
Dolly (2008)	27	963	85	Category 1
Edouard (2008)	14	996	55	Tropical Storm
Fay (2008)	50	986	60	Tropical Storm
Gustav (2008)	41	941	135	Category 4
Hanna (2008)	26	977	75	Category 1
Ike (2008)	31	935	125	Category 4
Paloma (2008)	32	944	125	Category 4
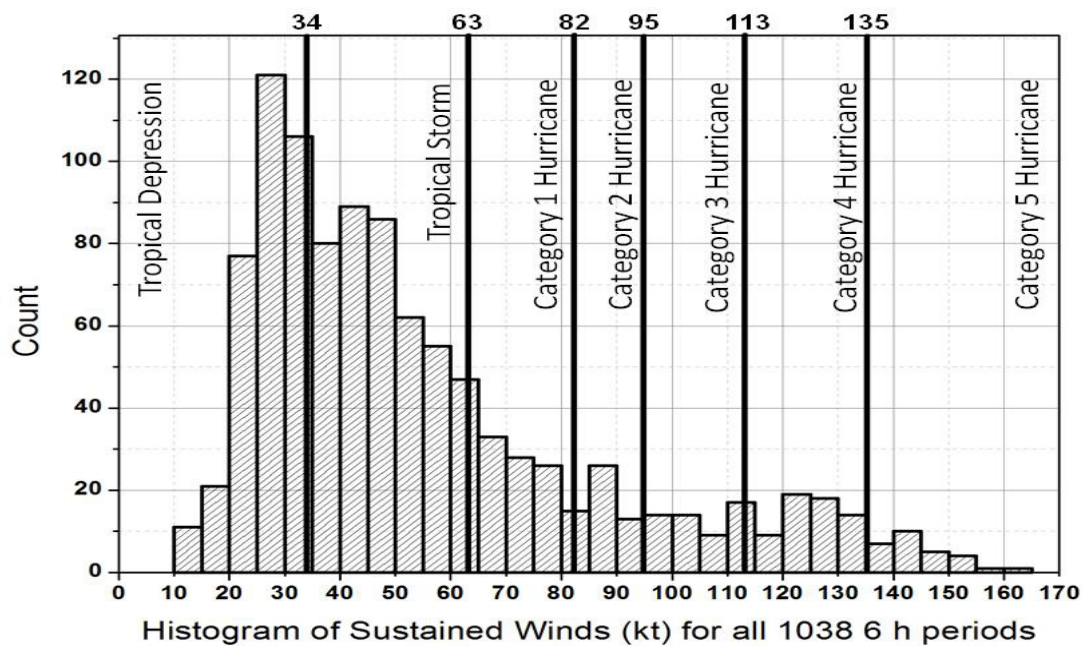
Figure 4. Frequency distribution of sustained wind speeds (kt) for all 1038 6 h periods

10

2.3 Lightning Density Distributions

To facilitate a comparison of our TC lightning distributions with those of prior studies (e.g., Lascody 1993; Lyons and Keen 1994; Samsury and Orville 1994; Molinari et al. 1994, 1999; Corbosiero and Molinari 2002, 2003; Molinari et al. 2004; Demetriades and Holle 2005, 2008; Demetriades et al. 2006, 2010; Abarca et al. 2010; Molinari and Vollaro 2010), polar flash density plots were prepared using OriginPro 8.1, a statistical software suite produced by OriginLab Company. To assess the variability in flash density with respect to storm intensity, flashes were subdivided into four categories (Fig. 3): Tropical depressions (TD), tropical storms (TS), category 1 and 2 hurricanes (C12), and category 3 and stronger hurricanes (C3+). We then created composite plots for each category. For example, if a storm exhibited TD force winds at a particular 6 h observation time, all flashes within a ± 3 h window were assigned to the TD group. Likewise, if that storm later became a category 5 hurricane, flashes for that period were placed in the C3+ group. These methods avoided focusing on just a few storms (case studies) and created a composite depiction of lightning with respect to intensity so that differences in CG flash distribution among the different TC intensity categories could be determined.

A similar method was adopted to study distributions of flash density among five intensity change thresholds as defined by changes in pressure tendency (Fig. 5). A pressure decrease of 10.5 hPa or greater during a 6 h period (42 hPa in 24 h) was defined rapid intensification (RI; NHC's glossary of NHC/TPC terms (2006)). Pressure falls between 5 and 10.5 hPa and 0 and 5 hPa in 6 h were classified fast intensification (FI) and slow intensification (SI), respectively. We also included a no pressure change (0 hPa in 6 h) and a weakening category for any 6 h period when pressure was rising. Fig. 5 shows that periods of no pressure change and weakening outnumber all periods of intensification.
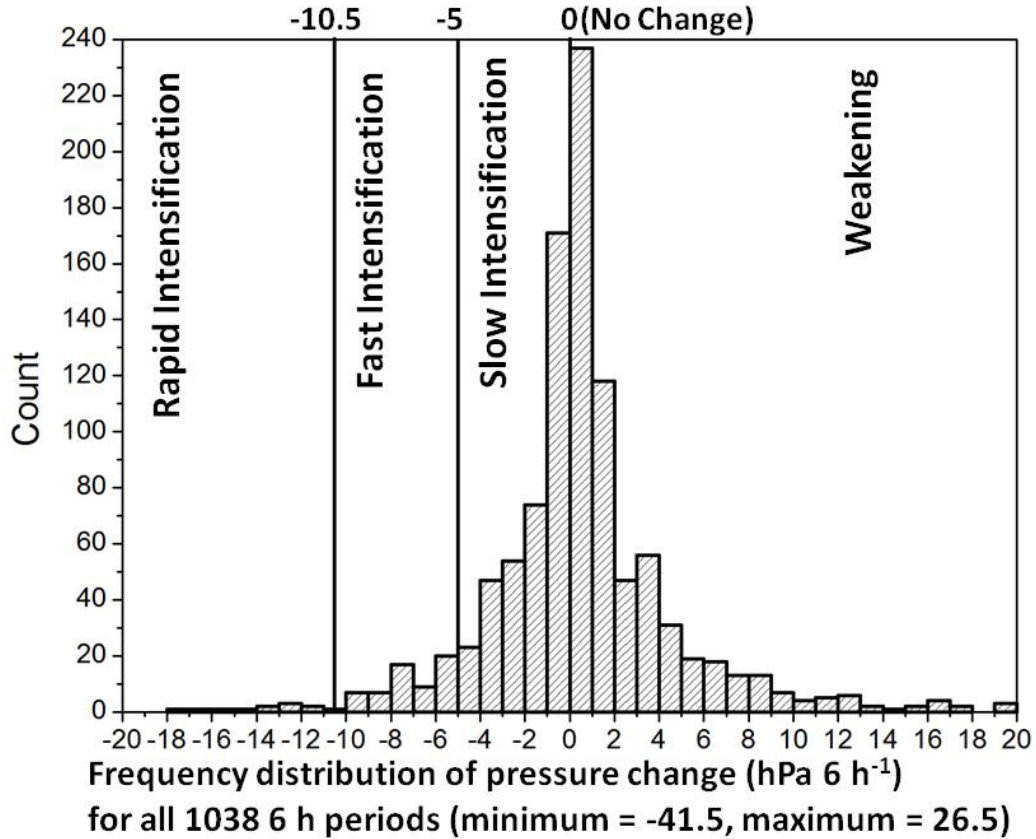
Figure 5. Frequency distributions of pressure change (hPa 6 h^{-1}) for all 1038 6 h periods.

Similar procedures were applied to storm motion (storm-relative coordinates) and deep-layer (850-200 hPa) vertical wind shear (shear-relative coordinates). Storm direction and speed were calculated between each 6 h best track latitude/longitude fix using a simple distance and bearing formula. Speeds were calculated using the computed distance between two consecutive 6 h positions. Following Corbosiero and Molinari (2003), the storm motion speeds were divided into three categories, slow (0-4 m s^{-1}), moderate (4-7 m s^{-1}), and fast (>7 m s^{-1}). Fig. 6 shows the distribution of storm speeds for the 1038 6 h observations, with the most common speed being ~ 4 m s^{-1}. To compute flash densities with respect to storm motion, all flash locations were rotated so the storm motion vector pointed due north (Corbosiero and Molinari 2002, 2003). This provided polar representations of flash densities at varying speeds and for varying storm intensities/intensification categories.

12
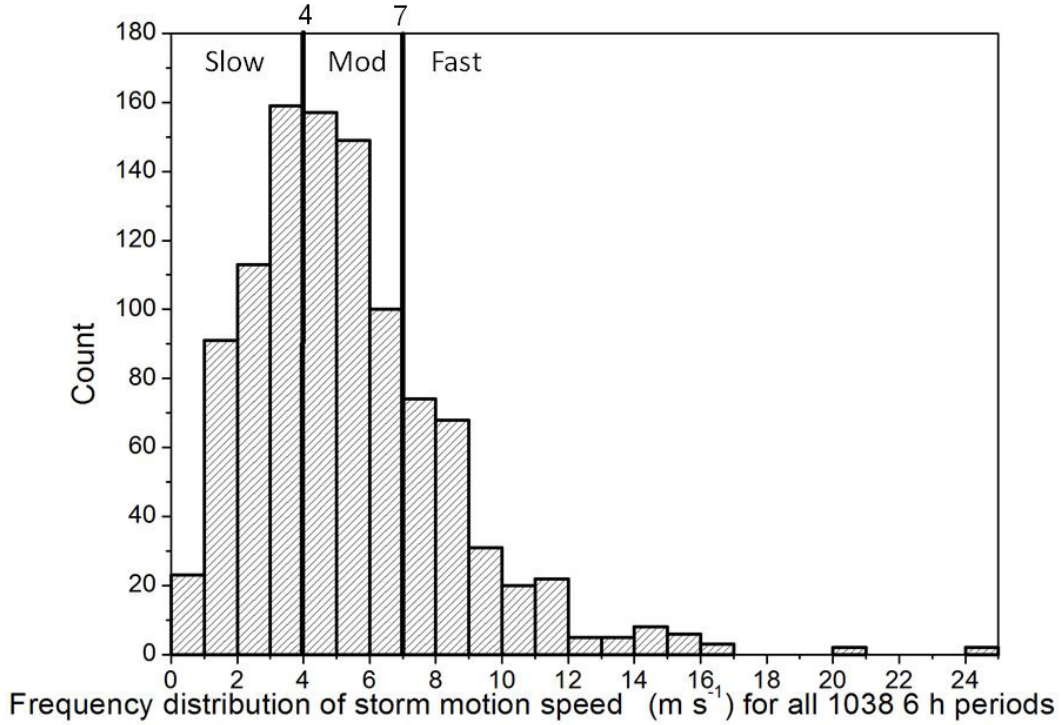
Figure 6. Frequency distribution of storm motion speed (m s^{-1}) for all 1038 6 h periods.

Deep layer wind shear was calculated for each 6 h period using the methodology of Molinari and Vollaro (1989), Hanley et al. (2001), and Corbosiero and Molinari (2002, 2003). GFS analyses were chosen for this purpose. This method removed a symmetric vortex by computing grids of area-weighted cylindrical Cartesian (U and V) wind components to diagnose the "across-storm flow" at various pressure levels. Following these calculations, the wind difference between 850 and 200 hPa was determined. Fig. 7 shows that the most common shear was ~ 7 m s^{-1}. Three categories of wind shear were defined to study lightning activity over a range of magnitudes. Weak wind shear was between 0 and 6 m s^{-1}, while moderate shear was between 6 and 9 m s^{-1} and strong shear greater than 9 m s^{-1}. Flash locations were rotated so the shear vector pointed due north (Corbosiero and Molinari 2002, 2003). Shear-relative flash density distributions were created for the various shear strengths, intensities, and periods of intensity change.
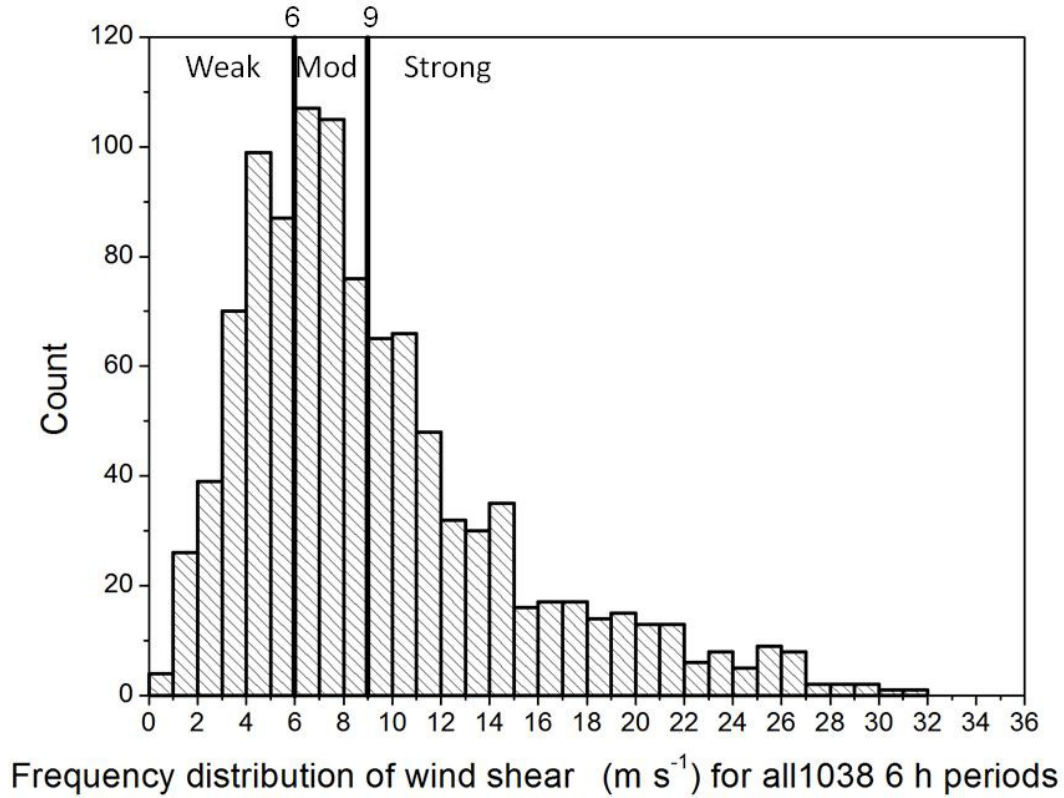
Figure 7. Frequency distribution of the 200-850 hPa vertical wind shear (m s^{-1}) for all 1038 6 h periods.

2.4 Correlations between Lightning and Intensity Change

Previous research mostly has consisted of case studies, describing lightning characteristics for only one or two storms at a time (Lascody 1993; Lyons an Keen 1994; Samsury and Orville 1994; Black and Hallett 1999; Squires and Businger 2008; Molinari and Vollaro 2010). The majority of these studies have focused on the relation between inner-core lightning and TC intensity (Lyons and Keen 1994; Samsury and Orville 1994; Molinari et al. 1999; Squires and Businger 2008). However, we consider lightning in additional regions of the TCs, as well as the relation between lightning and intensity change. Based on several previous studies (Molinari et al. 1999; Cecil et al. 2002a, b; Corbosiero and Molinari 2002, 2003; Squires and Businger 2008), we divided the TCs into three radial regions, the inner core (IC) within 100 km of the storm center, the outer rainbands (OR) between 100 and 300 km from the center, and the far outer bands (FOB) from 300 to 500 km. Although the 500 km value extends beyond the traditional bound of the OR zone (Molinari et al. 1999; Cecil et al. 2002a, b; Corbosiero and

Molinari 2002, 2003; Squires and Businger 2008), the results will show that the FOB region exhibits distinct variations of lightning that are related to the TC category and intensity change.

To obtain quantitative results regarding the nature of region-specific lightning and TC intensity, linear correlations (coefficients of determination - R^2) were calculated between lightning frequency and pressure change. Since we are exploring the potential utility of lightning observations in forecasting, flash rates were correlated with pressure change during three time frames, the pressure change period concurrent with the flash count, and the periods preceding and lagging the flash count. Correlations were assembled using both 6 and 3 h flash counts (Demetriades and Holle 2005, 2008; Demetriades et al. 2006, 2010) and 6 and 3 h interpolated pressures from the best-track data. Relationships between IC, OR, FOB, and storm-total (ST, 0-500 km) flash counts were compared for both 3 and 6 h to determine whether lightning was preferred in any region based on TC intensity (the TD, TS, C12, C3+, and RI designations). The resulting calculations provide insight into whether flash frequency in different regions of TCs can be related to intensity and/or intensity change. In addition to correlations, average 3 and 6 h flash rates and flash densities were computed for each category and radial region, similar to Demetriades and Holle (2008) who examined the inner core flash rates of Atlantic basin TCs between 2004 and 2007.

Price et al. (2009) correlated peak lightning activity derived from WWLLN data with maximum sustained wind speed in over 50 intense hurricanes (categories 4 and 5) around the world. To complement their study, we conducted a parallel diagnosis using our sample and the capabilities of the LLDN. For each storm, 6 h flash counts were correlated with wind speed at 6 h intervals out to ± 72 h (3 days). This yielded 24 lightning/wind speed correlations per storm, allowing us to evaluate longer term trends in lightning data.

CHAPTER 3

RESULTS

3.1 Lightning Flash Density Distributions

3.1.1 North-relative coordinates

We first describe spatial variations in lightning for each TC intensity category using north-relative coordinates. Lightning in each radial region is emphasized (inner core [IC]: 0-100 km, outer rainbands [OR]: 100-300 km, far outer bands [FOB]: 300-500 km, and storm total [ST]: 0-500 km). Fig. 8 shows composite north-relative CG flash density (flashes km^{-2} 6 h^{-1}) during periods of TD, TS, C12, and C3+ intensity. All values have been normalized by the number of 6 h periods per category (TD-336, TS-419, C12-155, C3+-128) yielding units of flashes km^{-2} 6 h^{-1}. It should be noted that flash density plots have not been normalized to account for flash activity in a given 6 h period. This means that a dominant 6 h period of lightning activity may mask the more consistent trend in flash density for a given categorical composite. In most cases however, our spatial findings are true to those of prior studies and can be regarded as reliable for general purposes.

The weaker storms (TDs and TSs) exhibit the most clustered and disorganized lightning pattern, with many flashes occurring within the IC. Conversely, the two hurricane groups have a more coherent lightning pattern with the C3+ category being most symmetric. Maximum lightning activity generally is located in the northeast and southeast quadrants and increases radially outward with storms of greater intensity. Although the TD and TS groups exhibit decreasing CG flash activity beyond ~350 km, the C12 and C3+ categories have substantial flash activity extending to 400 - 500 km.
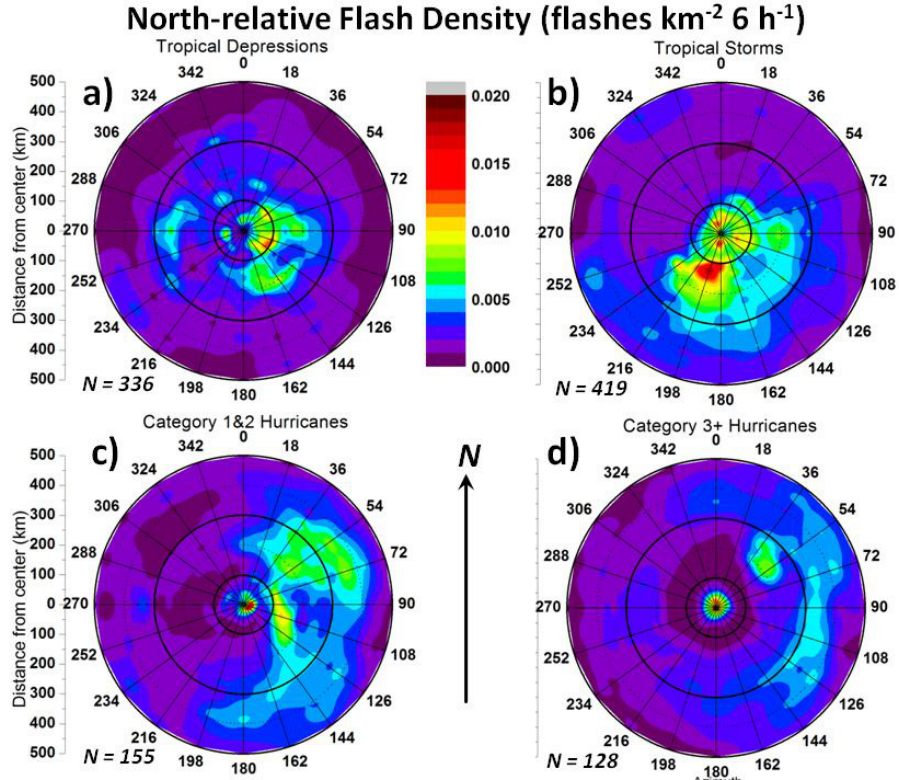
Figure 8. Plots of north-relative flash density (flashes km^{-2} 6 h^{-1}) in the 0-500 km radial range for a) tropical depressions, b) tropical storms, c) category 1 and 2 hurricanes, and d) category 3 and stronger hurricanes. Range rings are shown for the IC (100 km), OR (300 km), and FOB (500 km) regions. The number of 6 h periods (N) also is shown at the bottom left of each panel.

The IC region of each intensity category (Fig. 8) exhibits notable differences. TDs and TSs contain the most asymmetric IC lightning patterns. The C12 group contains a distinct IC signal with a slight tendency for flashes southeast of the center. Conversely, intense hurricanes (C3+) possess a nearly circular IC lightning pattern that coincides with the eyewall. The annular region of weak flash density between approximately 100 and 200 km in the C3+ storms corresponds to their inner rainband (Molinari et al. 1999, Cecil et al. 2002a, b). This area of small CG flash activity is where ice particles from deep eyewall convection descend to lower altitudes to create a stratiform shield of precipitation between the IC and OR structures (Molinari et al. 1999).

The TS category (Fig. 8b) contains the strongest flash densities over the greatest area, with maximum values ~ 0.02 flashes km^{-2} 6 h^{-1}. Demetriades and Holle (2008) concluded that average flash rates for TSs are greater than for other TC intensity categories, and current findings are

consistent with their results. Although the C12 and C3+ groups exhibit smaller areas of maximum flash densities, they are more azimuthally and radially organized.
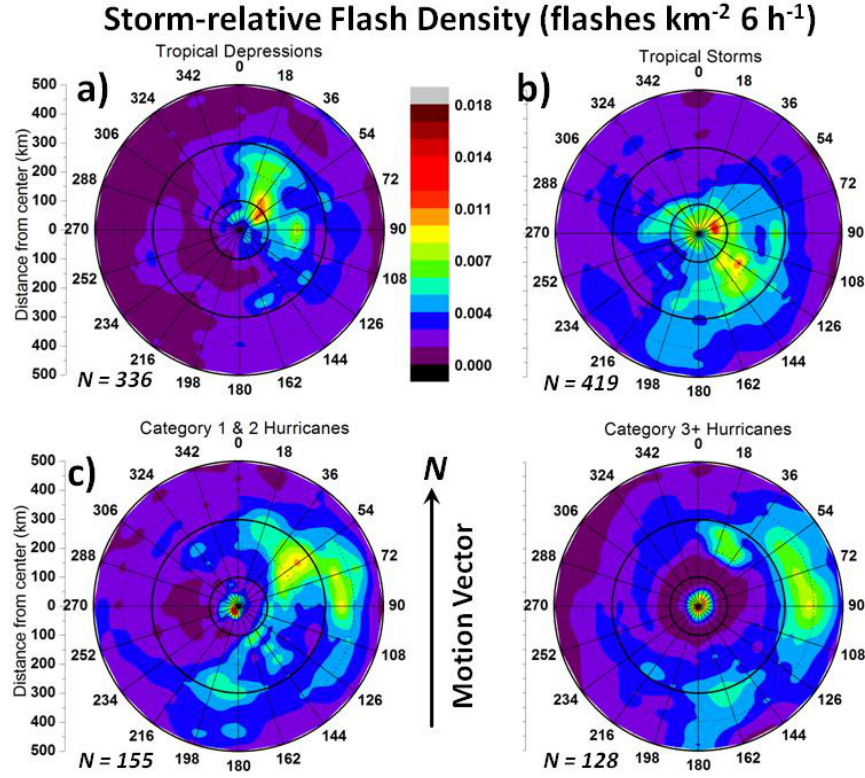
Figure 9. Storm-relative flash densities (flashes km^{-2} 6 h^{-1}) in the 0-500 km radial range for the a) TD, b) TS, c) C12, and d) C3+ intensity categories. The number of 6 h periods (N) also is shown at the bottom left of each panel.

Since there is some debate as to whether one should use the Cartesian (Fig. 8) or storm relative coordinate systems to depict lightning patterns (e.g., Corbosiero and Molinari. 2002, 2003, Abarca et al. 2010), we investigated both options. Fig. 9 displays flash densities in a storm-relative coordinate system with the motion vector pointing toward the top of each panel (toward the north). Results show most flashes located in the right front and rear quadrants of each TC intensity category. TDs exhibit a distinct flash maximum near the IC between 36 and 54º, with a broader region of flash density out to 300 km. The TS composite reveals maximum IC lightning between 36 and 90º, with a broader area of increased flash density in the OR region of the right rear quadrant. The C12 image shows greatest IC flash density in the left rear

18

quadrant. This unusual configuration is the result of hurricane Katrina (2005) that displayed unusually large flash rates in its southeast quadrant as it exited South Florida. Katrina was moving westward at this time, causing the flashes to appear in the left rear quadrant when the motion vector is oriented northward. This signature also was evident in the north-relative composite (Fig. 8c). The OR and FOB regions of C12 hurricanes contain greatest lightning in the right front quadrant. Finally, the C3+ distribution depicts a nearly symmetric IC signal. OR flash densities in these intense hurricanes are greatest in the right front quadrant, with maxima in the FOB located to the right of storm motion between the right rear and right front quadrants. The C12 and C3+ categories exhibit the greatest maximum flash densities (0.016 to 0.018 flashes km^{-2} $6 h^{-1}$), while the TS and TD groups contain weaker maximum flash densities of ~0.012 flashes km^{-2} $6 h^{-1}$.

To summarize, each motion relative plot (Fig. 9) displays maximum lightning densities in the IC region with secondary maxima in the OR/FOB areas. The stronger storms exhibit greater symmetry, with the C3+ distribution resembling the results of Molinari et al. (1994, 1999). The storm relative distributions (Fig. 9) exhibit many similarities to those of their north-relative counterparts (Fig. 8), with most lightning in the right front and rear quadrants. The C3+ category exhibits the same organized distribution in each coordinate system. Flash rotation with respect to storm motion mainly impacts the depiction of flashes in the IC region.

3.1.2 Forward motion-dependent relations

We next describe flash distributions with respect to storm forward speed (i.e., slow (0 - 4 m s^{-1}), moderate (4 - 7 m s^{-1}), and fast (> 7 m s^{-1})). Table 2 contains the sample size (number of 6 h observations), the number of different storms comprising each category, as well as the maximum number of 6 h observations attributed to a single storm (bold). Most TCs exhibit slow or moderate forward motion. TDs and TSs move relatively fast, with few hurricanes exhibiting fast forward motion. There are fewer samples of the stronger TC categories since hurricanes are less common than TDs and TSs.

Table 2. Sample size for all three storm motion categories. The number of 6 h observations is shown first. Inside the parentheses are the number of individual storms (plain text) and the maximum number of 6 h observations for a single storm (bold).

Category	Slow (0-4 m s^{-1})	Moderate (4-7 m s^{-1})	Fast (> 7 m s^{-1})
TD	121 (26-**16**)	126 (30-**13**)	89 (23-**11**)
TS	174 (31-**19**)	161 (32-**19**)	84 (24-**11**)
C12	58 (12-**15**)	63 (19-**12**)	34 (10-**8**)
C3+	33 (8-**15**)	56 (10-**18**)	39 (9-**11**)
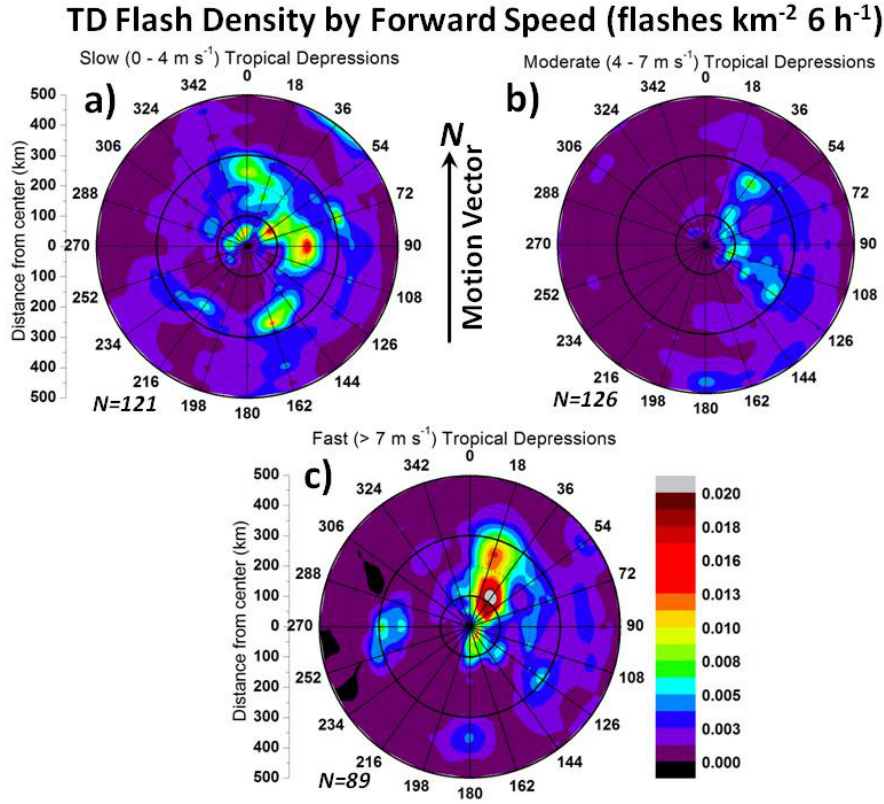
Figure 10. Storm-relative CG flash density (flashes km^{-2} 6 h^{-1}) in the 0-500 km radial range of the TD category during periods of a) slow, b) moderate, and c) fast forward motion. Range rings are shown for the IC (100 km), OR (300 km), and FOB (500 km) regions.

The most lightning in each forward speed category of TDs (Fig. 10) is located right of storm motion in the front and rear quadrants. Slow forward motion (0 – 4 m s^{-1}) produces more widespread lightning densities than moderate or fast movers. There are no well defined density centers during periods of moderate forward motion (4 – 7 m s^{-1}). For the fast moving TD category (> 7 m s^{-1}), maximum flash densities in the IC and OR regions are between 0 and 72°.

Table 3 shows that maximum flash densities for TDs are greatest for fast movers (~ 0.03 flashes km^{-2} 6 h^{-1}). Conversely, smallest maximum densities occur in the moderately paced TD group (0.011 flashes km^{-2} 6 h^{-1}).

Flash patterns for the three forward motion categories of TS systems (Fig. 11) are somewhat more organized than those of TDs (Fig. 10). Similar to the TDs, greatest flash activity generally is in the right front and right rear quadrants at all forward speeds. Flash density in the IC region is large in all cases, while OR and FOB density is greatest in the slow and moderate motion categories. Table 3 illustrates that maximum flash density at any grid point is greatest for the fast moving TSs (0.027 flashes km^{-1} 6 h^{-1}), with moderate moving TSs having the smallest maximum densities (~0.01 flashes km^{-1} 6 h^{-1}).
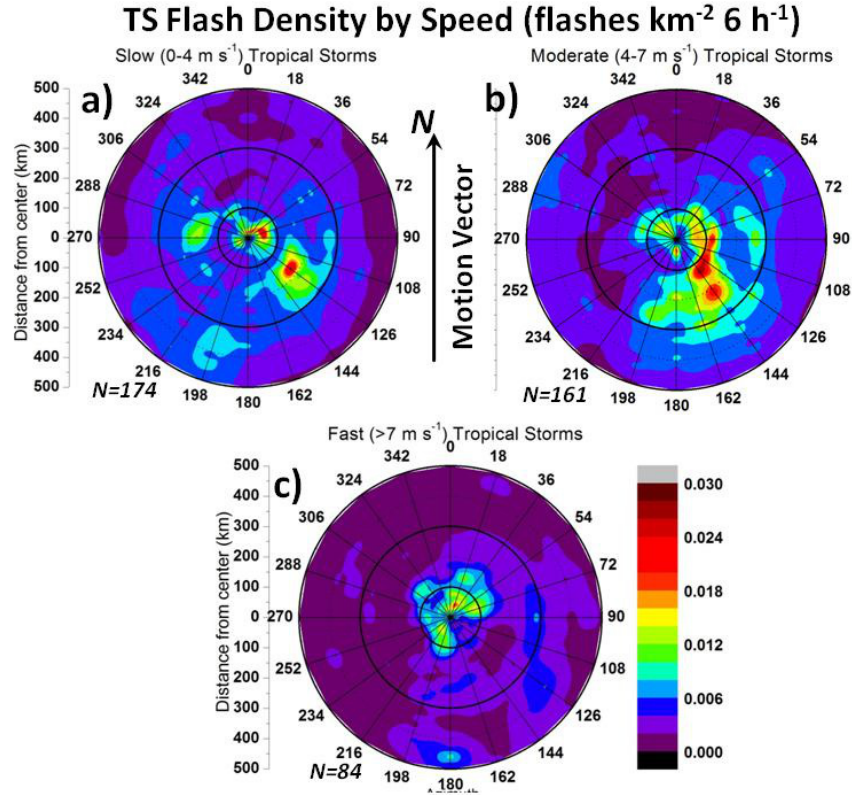
Figure 11. Storm-relative CG flash density (flashes km^{-2} 6 h^{-1}) in the 0-500 km radial range of the TS category during periods of a) slow, b) moderate, and c) fast forward motion
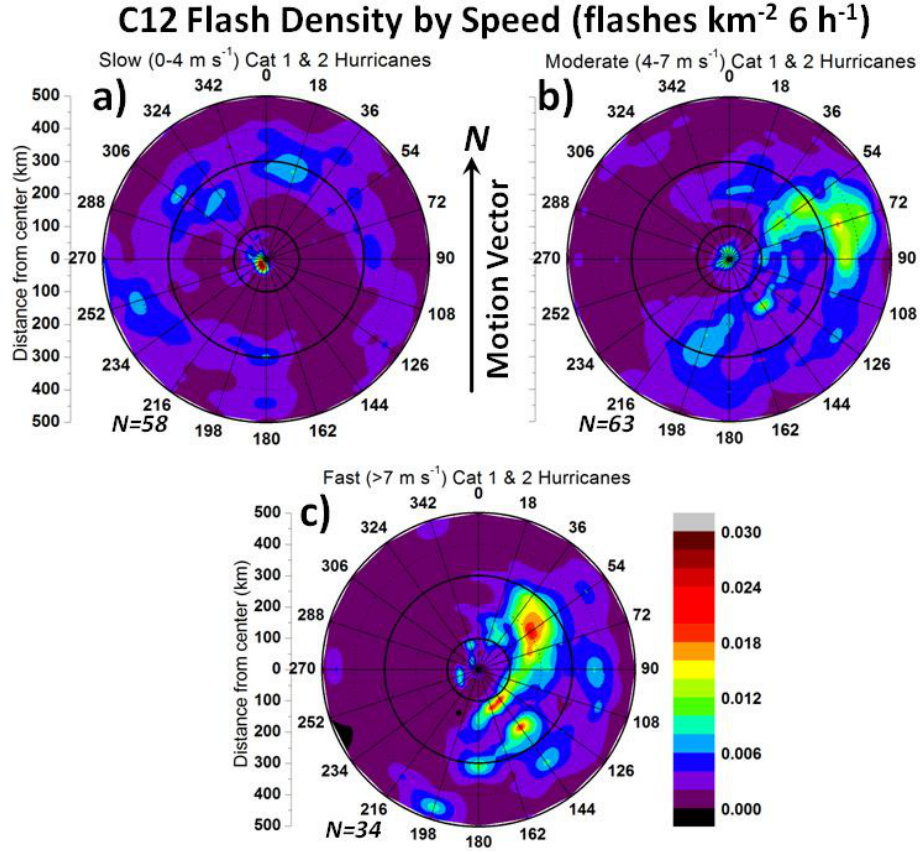
Figure 12. Storm-relative CG flash density (flashes km^{-2} 6 h^{-1}) in the 0-500 km radial range for the C12 category for periods of a) slow, b) moderate, and c) fast forward motion.

Table 3. Maximum flash densities (flashes km^{-2} 6 h^{-1}), and locations (IC, OR, FOB) for all forward motion-relative CG flash distributions.

Category	Slow (0-4 m s^{-1})	Moderate (4-7 m s^{-1})	Fast (> 7 m s^{-1})
TD	0.019 (OR)	0.011 (IC)	0.030 (OR)
TS	0.023 (OR)	0.015 (OR)	0.027 (IC)
C12	0.037 (IC)	0.020 (FOB)	0.023 (OR)
C3+	0.033 (IC)	0.015 (FOB)	0.021 (OR)

There is a clear distinction between flash distributions of the C12 group (Fig. 12 and 13) and the weaker categories discussed above (Figs. 10 and 11). The C12 densities exhibit the better organization that is characteristic of hurricanes (Fig. 12), with the OR and FOB regions more active than during TD/TS periods. Conversely, the IC region of C12 storms (Fig. 13) has smaller aerial flash density coverage than the TD and TS groups. The slow moving C12 group exhibits

greatest flash density in the left rear IC quadrant, and minimum flash density in both the right front and rear quadrants (Fig. 13a). This finding differs from some earlier studies regarding lightning and storm motion (Corbosiero and Molinari 2002, 2003, Abarca et al. 2010) and is due to hurricane Katrina (2005) that contained large amounts of lightning in the southeast quadrant (Fig. 8c) as it moved west over South Florida on 26-27 August, 2005. The majority of lightning in the moderate and fast motion categories is confined to the right two quadrants (Fig. 12b, c).Moderately paced C12 hurricanes show the most symmetric IC lightning pattern, while the slow and moderate paced C12 hurricanes exhibit more symmetry in the OR than fast moving storms. Contrary to the TD and TS groups whose maximum flash densities occur with the faster moving storms (Table 3), the C12 distribution exhibits greatest densities (0.037 flashes km^{-2} 6 h^{-1}) in the IC region of the slow motion category, with the moderate and fast categories having smaller maximum flash densities of ~ 0.020 flashes km^{-2} 6 h^{-1} in the OR and FOB regions.
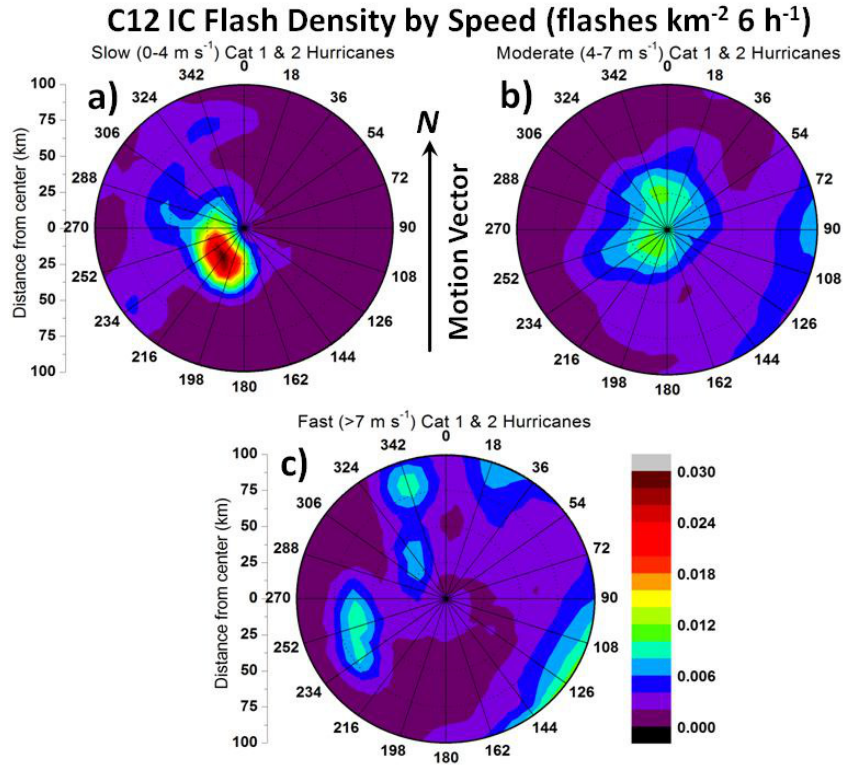
Figure 13. Storm-relative CG flash density (flashes km^{-2} 6 h^{-1}) in the 0-100 km (IC) radial range for the C12 category during periods of a) slow, b) moderate, and c) fast forward motion.

Finally, we assess lightning and forward speed relationships for intense hurricanes (C3+). This category exhibits the most organized flash distributions (Fig. 14), with distinct IC, OR and FOB signals at all forward speeds. The inner rainband is most evident in the moderate and fast paced groups. Densities in the OR and FOB regions are greatest in the fast-moving C3+ case. The slower C3+ systems contain more OR and FOB lightning in the right rear quadrant. This distribution rotates cyclonically to the right front quadrant with increasing forward speed.
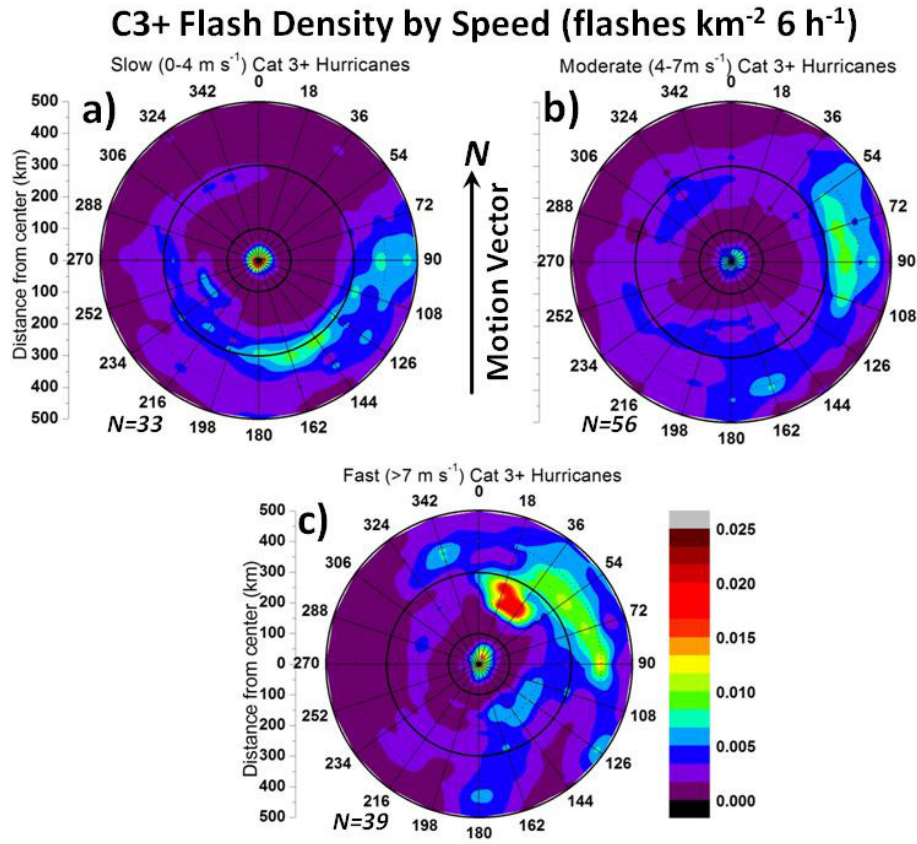
Figure 14. Storm-relative CG flash density (flashes km^{-2} 6 h^{-1}) in the 0-500 km radial range for the C3+ category for periods of a) slow, b) moderate, and c) fast forward motion.

Flash densities in the IC regions of C3+ storms (Fig. 15) reveal that faster storm speeds are associated with less IC flash symmetry. That is, slow moving intense hurricanes exhibit a nearly circular region of enhanced flash density within 50 km of the storm center, indicative of strong eyewall convection. The IC distribution of fast moving storms is more elliptical along the direction of motion. Slow C3+ periods display the greatest flash density (0.033 flashes km^{-2} 6 h^{-}

[1], Table 3), with fast-paced storms having maximum densities of ~ 0.02 flashes km^{-2} 6 h^{-1} and moderate storms having the smallest maximum flash densities (0.015 flashes km^{-2} 6 h^{-1}).
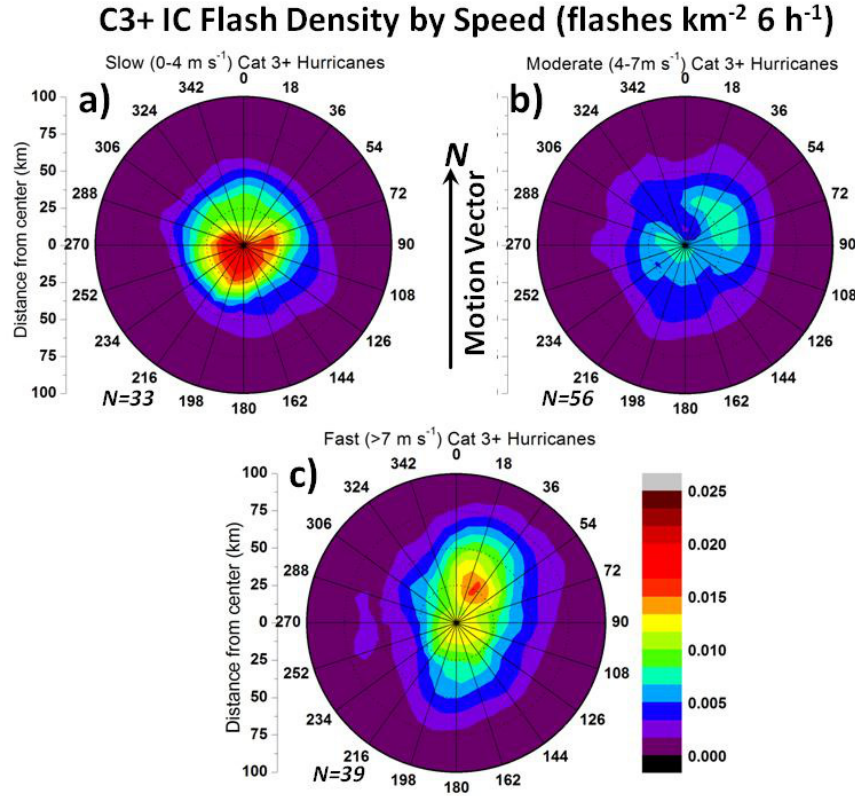
Figure 15. Storm-relative CG flash density (flashes km^{-2} 6 h^{-1}) in the 0-100 km (IC) radial range for the C3+ category during periods of a) slow, b) moderate, and c) fast forward motion.

To summarize, distributions of flash-density with respect to storm forward motion reveal interesting relationships. The TD and TS categories exhibit rather disorganized flash activity (Figs. 9-11). Increasing motion in these weaker storms results in decreased electrical activity at farther radii. This may be due partly to the typically smaller radii of TDs and TSs than the more intense TCs, but also may be linked to a lack of deep convection at further radii as forward motion increases (e.g., Corbosiero and Molinari 2003, Abarca et al. 2010). Conversely, the C12 and C3+ groups exhibit increasing lightning activity in the OR and FOB zones with increasing forward speed (Figs. 12-15). Their IC lightning is greatest when the forward motion is slow (Figs. 13a, 15a). Lightning asymmetries in the IC region are noted at moderate and fast forward

speeds as in Abarca et al. (2010). The two hurricane groups exhibit greatest maximum flash densities in the IC region, with smaller densities in the TD and TS composites which more often contain larger flash densities in the OR region. Lightning generally is preferred in the right front and right rear quadrants for all TC intensities.

3.1.3 Shear-relative relations

We next consider environmental impacts on TC lightning by analyzing the role of deep layer vertical wind shear (850 to 200 hPa). Corbosiero and Molinari (2003) and Abarca et al. (2010) noted that wind shear is more important in determining the orientation of lightning than is forward motion. Fig. 16 shows shear-relative flash densities of the four intensity categories, where each plot has been normalized by the number of 6 h periods comprising that category. Table 4 contains the number of 6 h observations for each shear and intensity classification as well as the number of different storms comprising each category and the maximum number of 6 h observations from the dominant storm. Sample sizes of the weaker intensity categories are greater than for hurricanes, but more TS and TD periods are in the strong shear category whereas hurricanes are nearly equally distributed among the three shear categories.

Table 4. Sample size for all three vertical wind shear categories. The number of 6 h observations is shown first. Inside the parentheses are the number of individual storms (plain text) and the maximum number of 6 h observations for a single storm (bold).

Category	Weak (0-6 m s^{-1})	Moderate (6-9 m s^{-1})	Strong (> 9 m s^{-1})
TD	90 (23-**11**)	74 (24-**7**)	172 (27-**20**)
TS	140 (31-**11**)	113 (29-**20**)	166 (32-**18**)
C12	50 (15-**9**)	55 (17-**7**)	50 (16-**13**)
C3+	45 (10-**11**)	46 (10-**8**)	37 (8-**11**)

Flashes in all categories (Fig. 16) are favored in the two downshear quadrants, consistent with Corbosiero and Molinari (2002, 2003), Abarca et al. (2010), and Molinari and Vollaro (2010). Lightning in the IC is greatest in the downshear-left quadrant in all but the TD group, shifting to downshear right in the OR and FOB regions. The TS category (Fig. 16b) clearly shows this relationship, with an area of enhanced flash density spiraling counterclockwise

toward the storm center. Both TDs and TSs feature small flash densities in their upshear quadrants, whereas hurricanes (Fig. 16c, d), with their generally better organized rainbands, exhibit some upshear lightning. Intense hurricanes (C3+) have the most symmetric lightning distribution (Fig. 16d). The TS and C12 composites contain the greatest maximum flash densities at any grid point (~0.02 flashes km^{-2} 6 h^{-1}), with the TD and C3+ flash densities exhibiting smaller maximum density values (~0.015 flashes km^{-2} 6 h^{-1}).
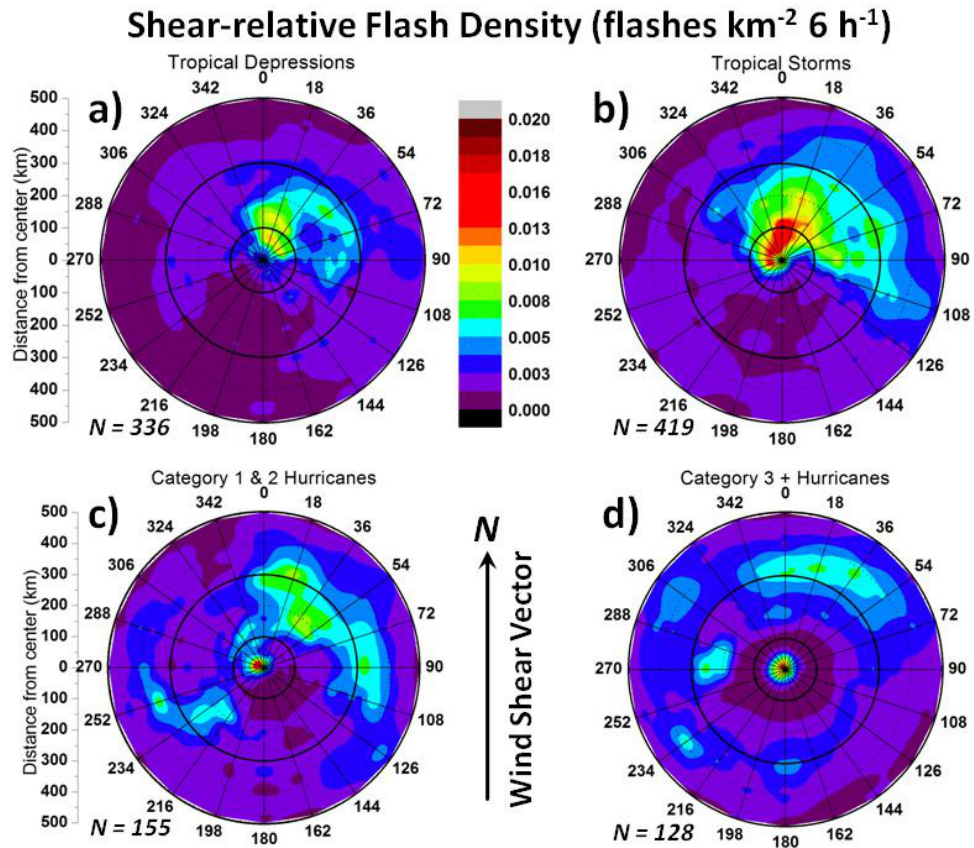
Figure 16. Shear-relative flash densities (flashes km^{-2} 6 h^{-1}) in the 0-500 km radial range for a) Tropical Depressions, b) Tropical Storms, c) Category 1 and 2 hurricanes, and d) Category 3+ hurricanes. The shear vector is oriented toward the top of each panel. Range rings are shown for the IC (100 km), OR (300 km), and FOB (500 km) regions. The number of 6 h periods (N) also is shown at the bottom left of each panel.

The shear-relative distributions (Fig. 16) are very different from their north-relative (Fig. 8) and storm-relative counterparts (Fig. 9), with differences most pronounced in the TS and C12

categories. The C3+ category contains the fewest differences between the three coordinate systems, with lightning associated with a symmetric eyewall, inner rainband, and outer rainband.
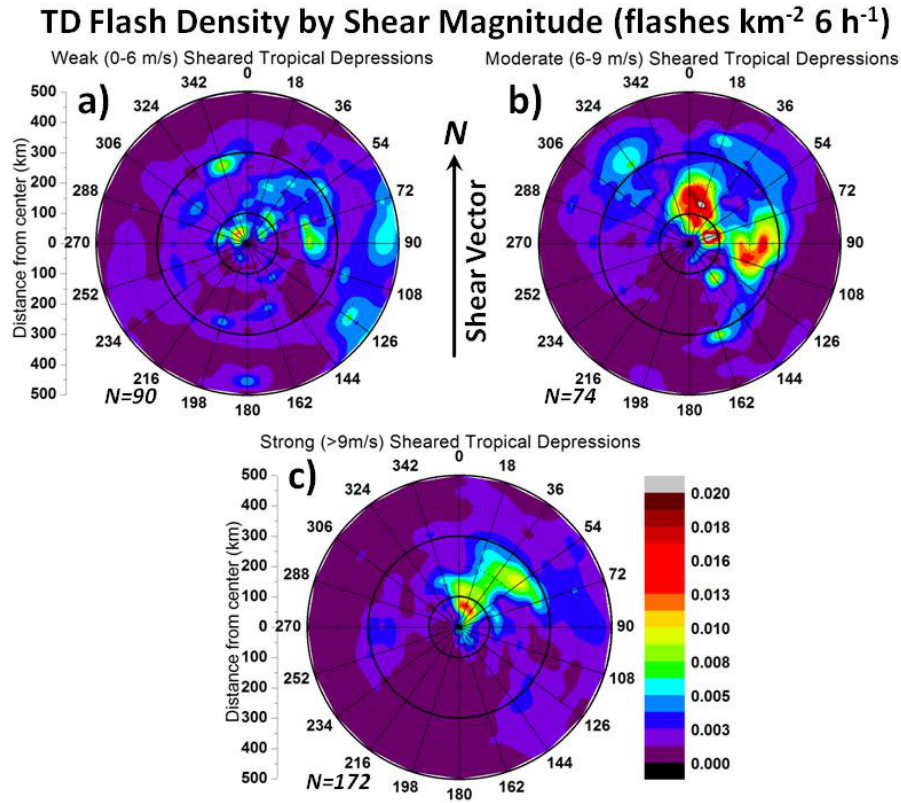
Figure 17. Shear-relative flash densities (flashes km^{-2} 6 h^{-1}) in the 0-500 km radial range for the TD category for a) weak, b) moderate, and c) strong wind shear. The shear vector is oriented toward the top of each panel.

Lightning patterns for TDs depend on the magnitude of vertical wind shear (Fig. 17). Moderate and strong shear induce a preference for lightning in the downshear right quadrant. However, weakly sheared TDs contain the most lightning in the downshear left quadrant. And, similar to fast-moving TDs (Fig. 10c), strong wind shear creates an azimuthal contraction in lightning activity (0-70°). Wind shear does not appear to impact the radial extent of flashes as much as did forward motion (Figs. 9a, 10a-c), with substantial flash activity extending out to the FOB region in all three shear magnitudes. Flash densities are greatest during moderate wind shear (~0.040 flashes km^{-2} 6 h^{-1}), with weak and strong shear producing smaller densities (0.014-

0.016 flashes km^{-2} 6 h^{-1}) (Table 5). Greatest densities are located in the IC region for all three shear categories.
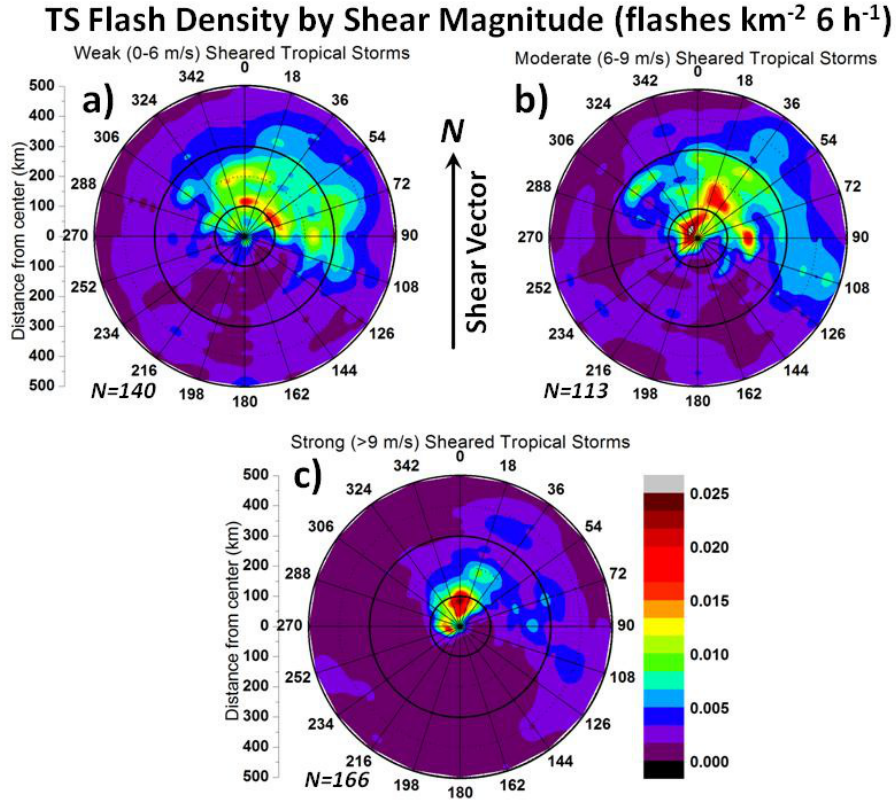
Figure 18. Shear-relative flash densities (flashes km^{-2} 6 h^{-1}) in the 0-500 km radial range of the TS category for a) weak, b) moderate, and c) strong vertical wind shear. The shear vector points toward the top of each panel.

TS periods (Fig. 18) exhibit stronger relationships between wind shear and lightning than did TDs (Fig. 17). A strong downshear preference is observed in all three shear categories, with little lightning in the upshear quadrants. Flash densities associated with weak shear display a widespread area of downshear lightning, while strongly-sheared storms contain larger densities, but through a smaller azimuthal range (300-45°). The OR/FOB regions exhibit enhanced lightning in each shear category, with large flash densities beyond 100 km; however, strong shear generates fewer OR/FOB flashes. Strongly-sheared TSs also exhibit a small IC flash maximum near 270 degrees that not seen in the OR and FOB regions. Although greatest flash densities are associated with moderate shear (~0.030 flashes km^{-2} 6 h^{-1}), densities for weak and

strong shear are only slightly less (Table 5). Maximum flash activity is in the IC for moderately and strongly sheared storms, but the weak shear category contains most lightning in the OR region.

Table 5. Maximum flash densities (flashes km^{-2} 6 h^{-1}) and locations (IC, OR, FOB) for all intensities and shear categories.

Category	Weak (0-6 m s^{-1})	Moderate (6-9 m s^{-1})	Strong (> 9 m s^{-1})
TD	0.016 (IC)	0.039 (IC)	0.014 (IC)
TS	0.023 (OR)	0.029 (IC)	0.026 (IC)
C12	0.032 (FOB)	0.041 (IC)	0.014 (IC)
C3+	0.027 (IC)	0.015 (IC)	0.015 (FOB)
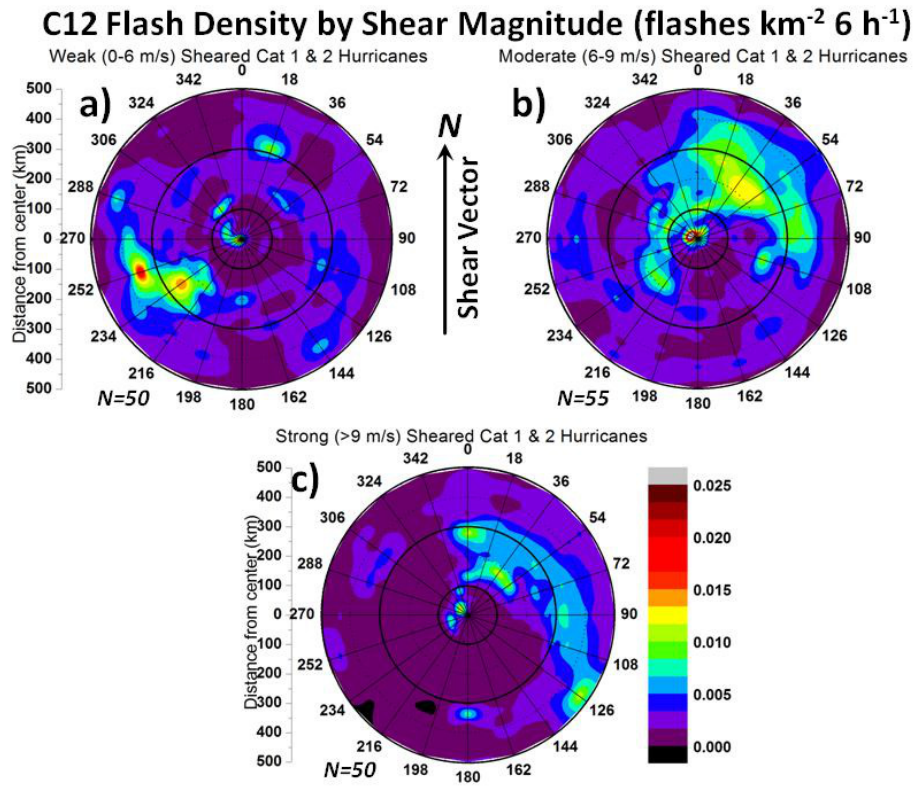
Figure 19. Shear-relative flash densities (flashes km^{-2} 6 h^{-1}) in the 0-500 km radial range of the C12 category during periods of a) weak, b) moderate, and c) strong vertical wind shear. The shear vector points toward the top of each panel.

Results for the two hurricane groups exhibit greater flash symmetry in all annular regions and a continued preference for lightning in the downshear quadrants (Figs. 19 and 20). Moderately sheared C12 storms produce the strongest OR and FOB densities (Fig. 19b), with weak and strong shear generating smaller signals (Fig. 19a, c). Fig. 20 shows that IC lightning is favored in the downshear left quadrants of both the moderate and strong shear categories, but there is an upshear left maximum during weak shear. Moderately sheared storms produce the greatest flash densities with weak shear producing the second greatest densities (Table 5). Maximum lightning density occurs in the FOB zone during weak shear, but in the IC region during moderate and strong shear.
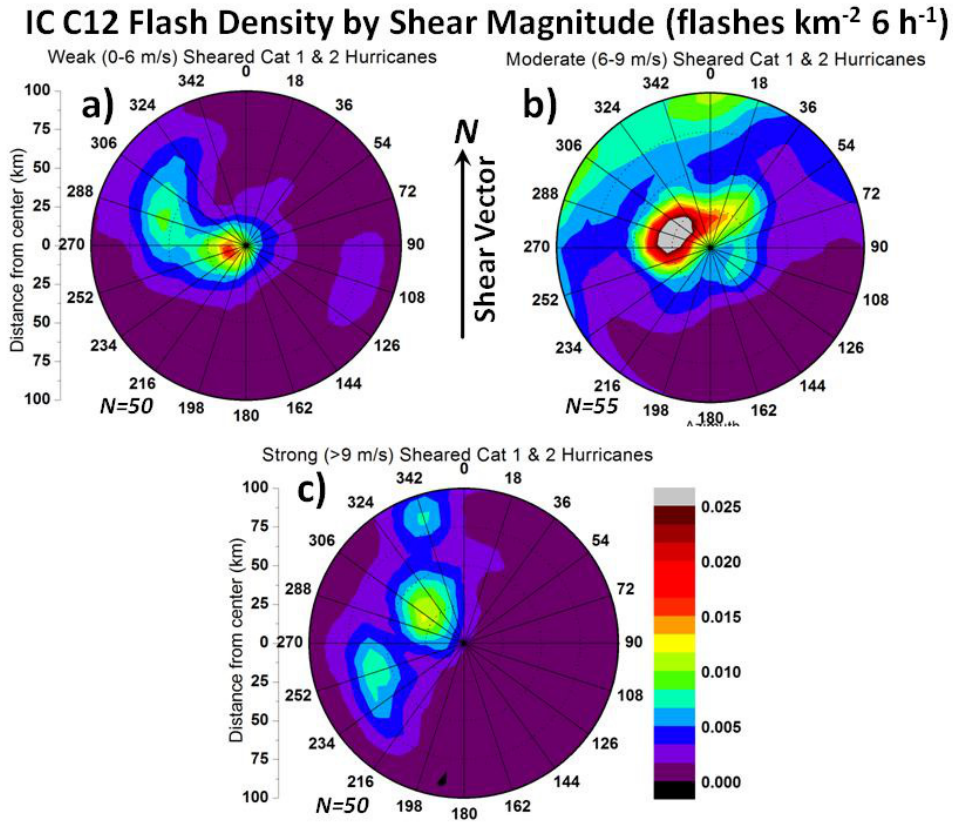
Figure 20. Shear-relative flash densities (flashes km^{-2} 6 h^{-1}) in the 0-100 km (IC) radial range for the C12 category during periods of a) weak, b) moderate, and c) strong vertical wind shear. The shear vector points toward the top of each panel.

Intense hurricanes (C3+) exhibit well organized lightning distributions in all three shear categories (Figs. 21 and 22). An inner rainband signal is seen in each shear category, and large

lightning densities are evident in the OR and FOB areas (Fig. 21) with an inner rainband signal in each shear category. Weak shear produces the most symmetric presentation. Then, as wind shear increases to moderate and strong, lightning in the OR/FOB regions becomes more confined to the downshear right quadrant. IC lightning (Fig. 22) is greatest in the downshear left quadrant in all three shear categories. Weak shear produces greatest flash densities in the IC (0.027 flashes km^{-2} 6 h^{-1}, Table 5), with moderately and strongly sheared storms having nearly equal maximum densities (~ 0.015 flashes km^{-2} 6 h^{-1}) in the IC and FOB regions.
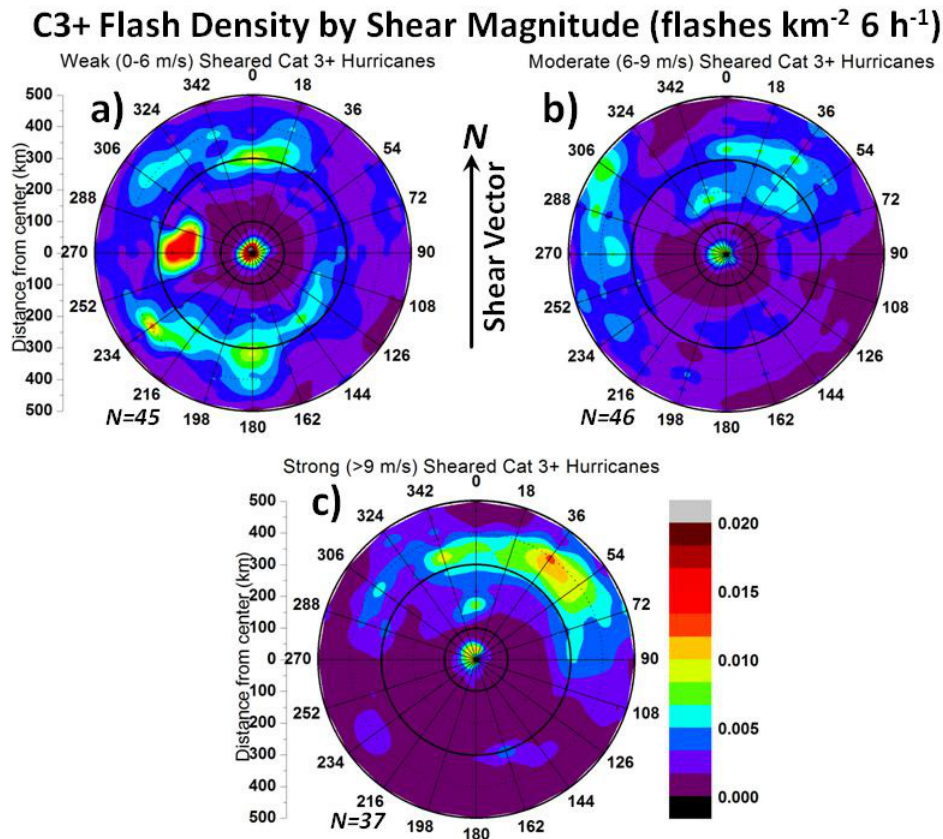
Figure 21. Shear-relative flash densities (flashes km^{-2} 6 h^{-1}) in the 0-500 km radial range of the C3+ category during periods of a) weak, b) moderate, and c) strong vertical wind shear. The shear vector points toward the top of each panel.
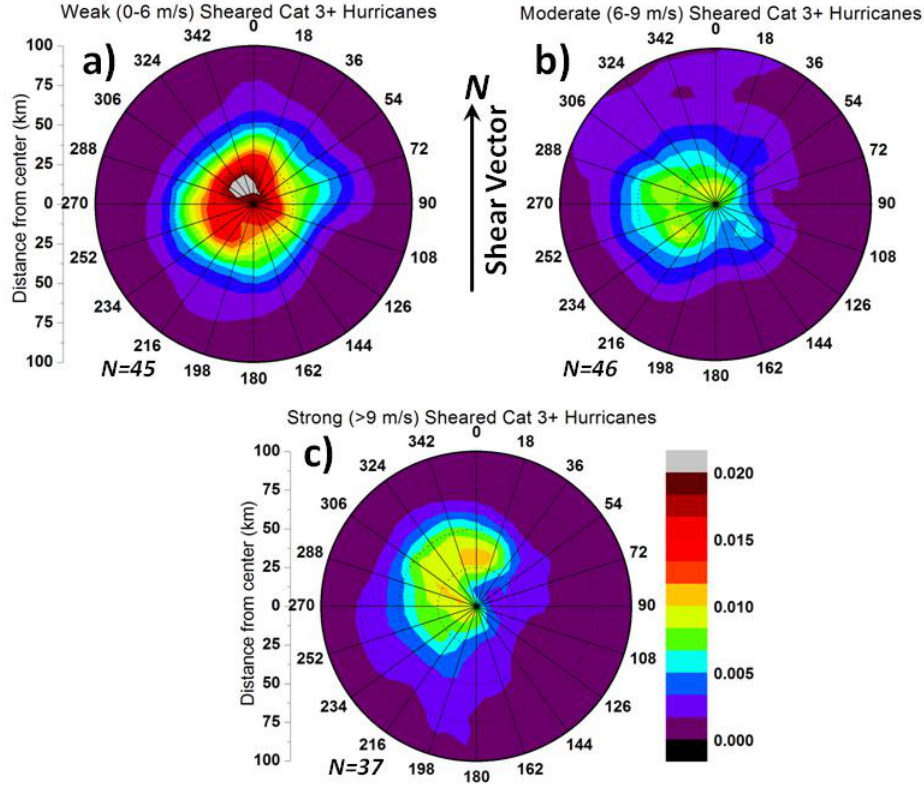
Figure 22. IC Shear-relative flash densities (flashes km^{-2} 6 h^{-1}) in the 0-100 km (IC) radial range for the C3+ category during periods of a) weak, b) moderate, and c) strong vertical wind shear. The shear vector points toward the top of each panel.

Several general relationships are apparent in the plots of shear-relative flash density. Lightning is most common in the two downshear quadrants of most TC intensities and all magnitudes of wind shear (Fig. 16 – 22). Lightning in the IC (OR/FOB) region is most prevalent in the downshear left (right) quadrant. Previous studies have shown similar results (Corbosiero and Molinari 2002, 2003; Abarca et al. 2010; Molinari and Vollaro 2010). Frank and Ritchie (2001) simulated the effects of wind shear on numerically simulated hurricanes. They found that maximum convection and reflectivity were located to the left of shear, arguing that shear-induced vorticity advection generated low-level convergence downshear and to the left. Reasor et al. (2004) similarly, showed that IC convection reverses the vortex tilting that is due to wind shear. Since the shear vector is oriented northward in our depictions, resilience to tilting requires that deep convection occur downshear and to the left of the shear vector in order to be advected

33

cyclonically against the shear. Simulations of hurricanes Bonnie (1998) and Erin (2001) (Braun et al. 2006, Braun and Wu 2007) produced intense eyewall updrafts in the downtilt (downshear) quadrants. These updrafts were enhanced by eyewall mesovortices interacting with the storm-relative flow in the downshear quadrants. The updrafts weakened as they circulated upshear against the tilt. Eastin et al. (2005) found that the most buoyant updrafts in a number of hurricane eyewalls were located left of shear (downshear). These results support the left of downshear flash density maximum in the IC of hurricanes and to a lesser extent in the weaker TCs. TDs appear to be the least resilient to wind shear exhibiting a downshear right lightning maximum except during cases of weak shear. Resilience to vortex tilting appears to be optimized during weak and moderate shear, but as shear exceeds 9 m s^{-1}, deep convection is less likely to persist, yielding smaller average flash densities.

3.1.4 Intensity change relations

We next examine flash densities for five magnitudes of TC pressure change to determine if fluctuations in lightning are related to changes in TC intensity. NHC defines RI as a decrease in pressure of 42 hPa or more during a 24 h period, corresponding to a 10.5 hPa decrease in 6 h (5.25 hPa in 3 h - NHC's glossary of NHC/TPC terms (2006)). Four other pressure change categories also were defined (slow intensification (SI) -5 to 0 hPa 6 h^{-1}, fast intensification (FI) -10.5 to -5 hPa 6 h^{-1}, no pressure change, and weakening). The number of 6 h periods and the number of storms in each category are shown in Table 6. The most frequent intensity changes are weakening and SI (807 6 h periods; 77% of the observations). The smallest samples are the FI (71 6 h periods) and RI (15 6 h periods) groups that together comprise only ~8% of the sample.

Table 6. Sample size for the five intensity change groups (number of 6 h periods) and the number of individual storms in each group. The number of 6 h observations from a single storm is bold in parenthesis.

Intensity Change	Number of 6 h periods	Number of Storms
Weakening (>0 hPa 6 h^{-1})	449	44 (**33**)
No Pressure Change (0 hPa 6 h^{-1})	145	36 (**13**)
Slow Intensification (-5 to 0 hPa 6 h^{-1})	358	42 (**18**)
Fast Intensification (-10.5 to -5 hPa 6 h^{-1})	71	25 (**8**)
Rapid Intensification (< -10.5 hPa 6 h^{-1})	15	7 (**4**)

34

Flash Density by Pressure Change (flashes km^{-2} 6 h^{-1})
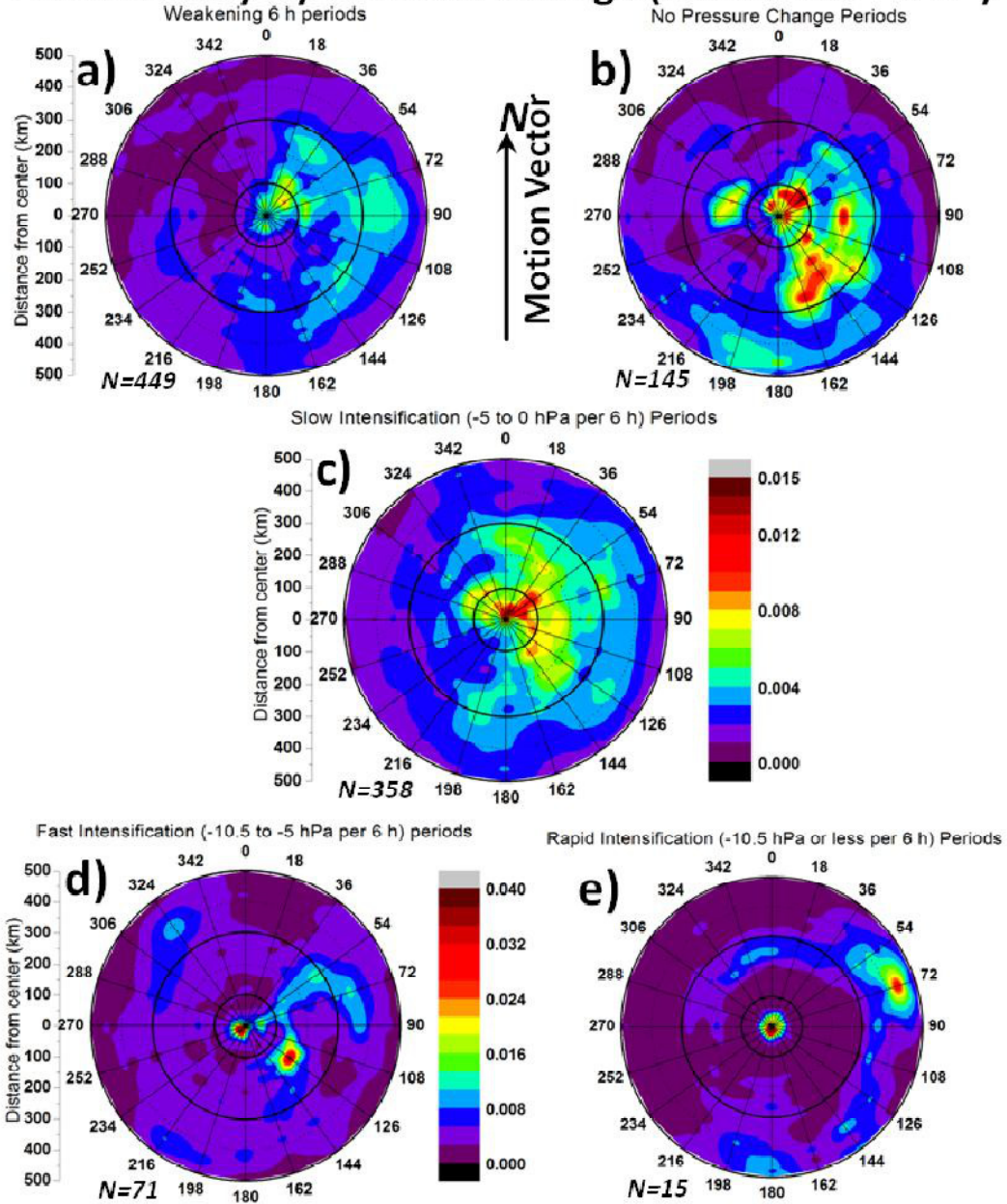
Figure 23. Storm-relative flash densities (flashes km^{-2} 6 h^{-1}) in the 0-500 km radial range during periods of a) weakening, b) no pressure change, c) slow intensification, d) fast intensification, and e) rapid intensification. The shear vector points toward the top of each panel. Note the different color scales between the top three and bottom two categories. The number of 6 h periods (N) also is shown at the bottom left of each panel.

Figure 24. Storm-relative IC flash densities (flashes km^{-2} 6 h^{-1}) in the 0-100 km (IC) radial range during periods of a) fast intensification and b) rapid intensification, The motion vector is oriented toward the top of each panel.

Storm-relative flash densities for all five intensity change categories in the 0-500 km radial range are shown in Fig. 23. Flash maxima during weakening, no change, or slow intensification (Fig. 21a-c) are in the right front and right rear quadrants. However, during FI and RI, density maxima are more confined to the IC and to greater distance than observed in the weaker categories of pressure change (Figs. 23d, e, 24). This confinement is due partly to the smaller sample sizes. The preference for lightning in the left rear quadrant during FI is due to hurricane Katrina (2005) (Figs. 8, 9, 12 and 13) that intensified quickly as it moved into the Gulf of Mexico and contained a single highly active 6 h period of lightning.

Table 7. Maximum flash density (flashes km^{-2} 6 h^{-1}) and their locations for all storm-relative intensity change composites.

Intensity Change	Maximum Density (flashes km^{-2} 6 h^{-1})	Region (IC,OR,FOB)
Weakening (>0 hPa 6 h^{-1})	0.010	IC
No Pressure Change (0 hPa 6 h^{-1})	0.017	IC
Slow Intensification (-5 to 0 hPa 6 h^{-1})	0.016	IC
Fast Intensification (-10.5 to -5 hPa 6 h^{-1})	0.046	IC
Rapid Intensification (< -10.5 hPa 6 h^{-1})	0.059	IC

Table 7 lists maximum flash densities and their associated regions for the five intensification groups. Weakening storms exhibit the smallest maximum storm-relative flash density, with periods of no pressure change and SI having similarly small maxima. Maximum flash density increases ~300% between the three weaker categories and the FI/RI periods. This is an important finding about the nature of lightning during FI and RI periods. Maximum densities in all pressure change categories occur in the IC region (Fig. 23 and 24). Since IC lightning is greatest during periods of greater pressure falls, IC flash activity may be a method for monitoring intensification. This potential is considered further in the following section.

Current results considering storm motion and vertical wind shear show many similarities to previous studies (Corbosiero and Molinari 2002, 2003; Abarca et al. 2010). Our findings go further to reveal a preference for right of motion lightning during the weakening, no-pressure change, and SI periods (Fig. 23). The FI and RI periods differ by exhibiting greater flash maxima in the IC (Fig. 24), with a preference for lightning in the left rear quadrant during FI and nearly symmetric about the IC during RI (Fig. 24).

We next relate intensity change to shear-relative flash density. A previous section showed that lightning was most common in the downshear left IC region (Corbosiero and Molinari 2002, 2003; Eastin et al. 2005; Braun et al. 2006, Braun and Wu 2007; Abarca et al. 2010; Molinari and Vollaro 2010), especially during periods of TS, C12, and C3+ intensity. Results show that this relationship continues when considering pressure change.

Figure 25 relates flash distributions for the five pressure change categories to the vertical wind shear. During periods of weakening, IC lightning is greatest directly downshear, whereas periods of no pressure change and SI show broader IC flash densities that spread in the downshear left and right directions. The tendency for lightning to remain directly downshear in weakening systems has not been shown previously. Shear-induced vortex tilting of weakening storms causes deep IC convection to advect directly downshear, inducing greater flash densities in this region. Storms with constant pressure or SI are more resilient to wind shear; thus, the arguments of Frank and Ritchie (2001) and Reasor et al. (2004) apply to the downshear left IC lightning signal.

37
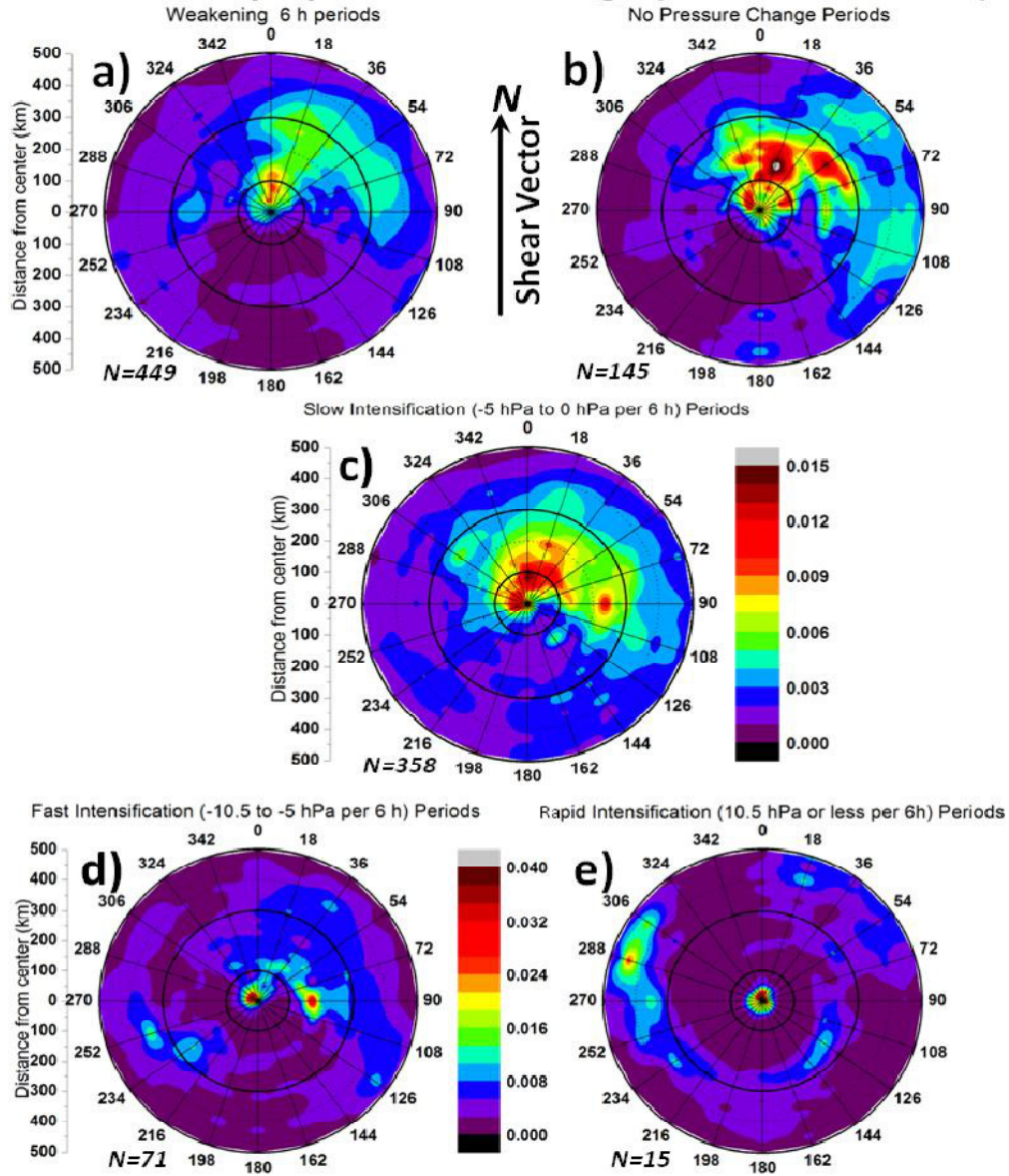
Figure 25. Shear-relative flash densities (flashes km^{-2} 6 h^{-1}) during periods of a) weakening, b) no pressure change, c) slow intensification, d) fast intensification, and e) rapid intensification. The shear vector points toward the top of each panel. Note the different color scales between the top three and bottom two categories.

In the case of stronger intensification (Figs. 25d-e, 26), the inner core generally is more active than the OR and FOB regions. Lightning in the OR and FOB regions is most common in the downshear-right (left) quadrant during FI (RI). RI periods continue to display the inner

rainband noted by Molinari et al. (1994, 1999). This occurs primarily because most TCs undergoing RI become C3+ storms when the inner rainband is frequently observed. Flash densities in the IC (Fig. 26) are greatest in the downshear left quadrant for both intensification categories as observed by Corbosiero and Molinari (2002, 2003), Eastin et al. (2005), Braun et al. (2006), Braun and Wu (2007), Abarca et al. (2010), and Molinari and Vollaro (2010). This location is believed to be the result of convection attempting to maintain the vertical vortex against the wind shear (Reasor et al. 2004).
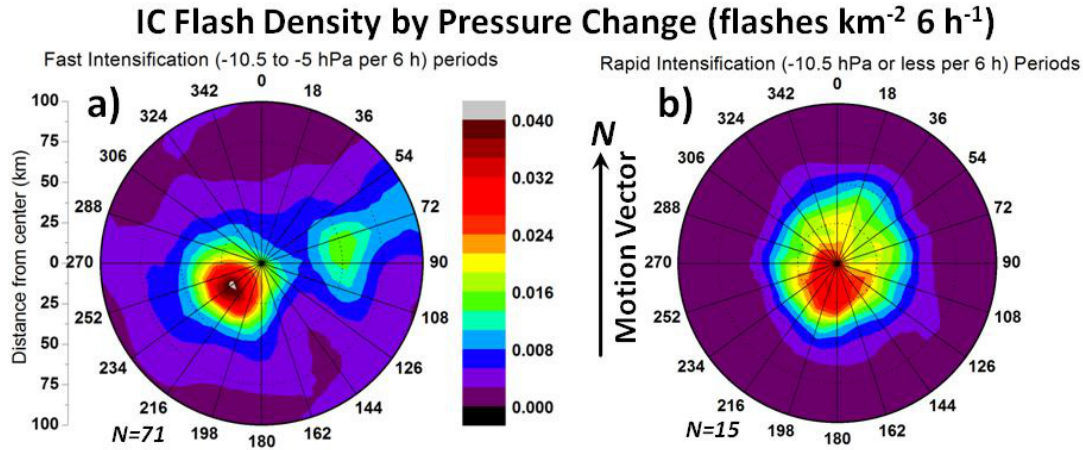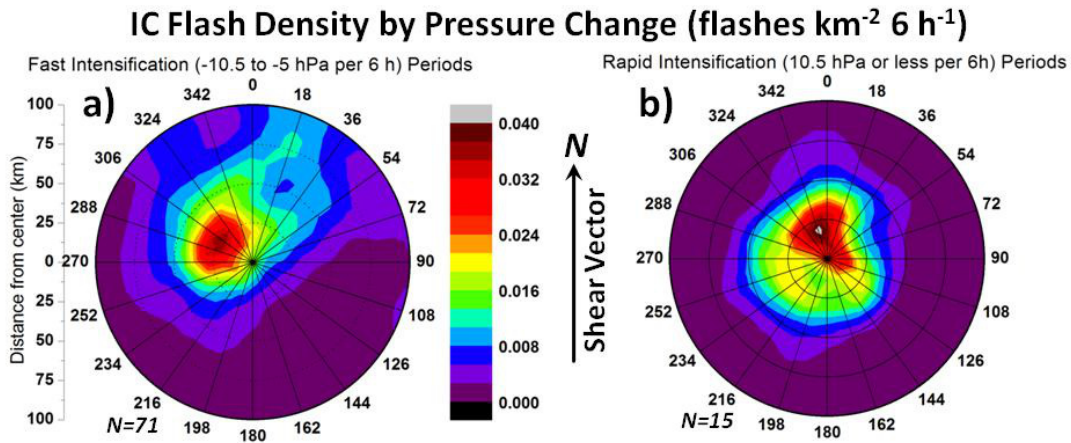

Figure 26. Shear-relative IC flash densities (flashes km^{-2} 6 h^{-1}) in the 0-100 km (IC) radial range during periods of a) fast intensification and b) rapid intensification, The shear vector is oriented toward the top of each panel.

Table 8 displays the greatest shear-relative flash densities at any grid point and locations of this greatest density. Periods of SI, no change, and slow strengthening exhibit similarly small maximum flash densities. Maximum flash densities increase greatly between the first three pressure change groups and the FI/RI periods. Maximum flash densities move inward toward the IC region for the three intensification periods (SI, FI, RI). Thus, there is a clear preference for greater flash activity in the IC region during all periods of intensification.

Table 8. Maximum flash density (flashes km^{-2} 6 h^{-1}) and locations for all shear-relative intensity change composites.

Intensity Change	Maximum Density (flashes km^{-2} 6 h^{-1})	Region (IC,OR,FOB)
Weakening (>0 hPa 6 h^{-1})	0.010	IC/OR
No Pressure Change (0 hPa 6 h^{-1})	0.016	OR
Slow Intensification (-5 to 0 hPa 6 h^{-1})	0.015	IC
Fast Intensification (-10.5 to -5 hPa 6 h^{-1})	0.040	IC
Rapid Intensification (< -10.5 hPa 6 h^{-1})	0.050	IC

Findings in the various pressure change categories (Figs. 23-26) are similar to those observed in the vertical wind shear and motion-relative flash distributions (Figs. 8-22). Storm-relative distributions reveal a preference for lightning in the right front and rear quadrants during periods of weakening, no pressure change, and SI. However, distributions during periods of FI and RI are different, with most lightning occurring in the right and left rear quadrants and in the IC region. Lightning in the OR and FOB regions is more common in the weakening, no pressure change, and SI groups. However, IC flash activity increases in the strongest intensification categories. With respect to wind shear, the downshear left (right) quadrant contains the most IC (OR) lightning. During weakening periods, shear displaces most IC convection and lightning directly downshear, between the downshear right and left quadrants.

3.2 Quantitative Lightning Relations

3.2.1 Average Categorical Flash Rates

While the previous distributions contain valuable clues relating lightning patterns to storm motion, wind shear, and intensification, a more quantitative analysis is needed to determine whether lightning in specific regions of a TC is related to intensity change. We computed average flash rates and densities over 3 h and 6 h intervals in each annular region (IC, OR, FOB, ST 0-500 km) of each intensity category. Corrections were applied to the raw CG flash counts to account for geographical variations in the DE (Fig. 2) following Demetriades and Holle (2008). Demetriades and Holle (2008) showed that CG flash rates in TCs tend to be greatest prior to landfall and decrease once the storm is positioned inland. Thus, to avoid the possible effects of land masses on average flash rates, all periods when TC centers were located

over land were removed from the calculations. This yielded a total sample of 1458 and 740 periods for 3 and 6 h intervals, respectively. Average flash rates also were computed during periods of RI.

Tables 9 and 10 contain average 3 and 6 h flash rates and flash densities (flashes km^{-2}) for each TC intensity category and during periods of RI. Storm total (0-500 km) flash rates and densities at both time intervals are similar for the TS, C12, and C3+ groups. There is no clear tendency for strong storms to produce more lightning. However, TDs do exhibit considerably smaller flash rates, while the RI groups display the greatest rates and flash densities. Lightning in the OR region averages ~ 600 flashes 3 h^{-1} (~0.0024 flashes km^{-2} 3 h^{-1}) (~1200 flashes 6 h^{-1} (~0.0050 flashes km^{-2} 6 h^{-1})) for all intensity categories except TSs which produce the greatest OR flash rates/densities (741 flashes 3 h^{-1} (~0.0029 flashes km^{-2} 3 h^{-1}) and ~1500 flashes 6 h^{-1} (~0.0059 flashes km^{-2} 6 h^{-1}), respectively). Moving further outward, the FOB region shows a clear increase in flash rate and flash density with greater intensity. The greatest increase occurs between the TD and TS periods for both 3 and 6 h when flash rates increase ~60%. Thus, the relatively distant FOB region should be considered when documenting the electrical characteristics of TCs.

Periods of RI produce the greatest average flash rates and densities for both time intervals (Tables 9 and 10). In the IC region, average 3 and 6 h flash rates/densities are greatest during TS and TD intensity, decreasing to a minimum during C3+ periods. The IC region produces the smallest average 3 and 6 h flash rates, but when the relatively small area of the IC is considered, it exhibits the greatest average flash density, except for C3+ hurricanes. Conversely, the OR and FOB regions contain the greatest number of flashes, but have smaller flash densities due to their larger areas, especially for the TD and TS intensities. Flash rates and densities in the IC during RI are greater than during the two hurricane periods, but not as strong as during TS intensity. Nonetheless, RI generally is associated with enhanced IC lightning. These findings are consistent with those of Demetriades and Holle (2008) and Demetriades et al. (2010) who found that TSs produce the greatest average IC flash rates, with the stronger hurricanes having smaller IC flash rates.

Table 9. Average 3-h flash rates for all categories and radial regions; with 3 h flash densities ((flashes km^{-2} 3 h^{-1}) $\times$ 10^{-3}) in parentheses.

Category	Sample Size	Storm Total 0-500 km	Inner Core 0-100 km	Outer Rainbands 100-300 km	Far Outer Bands 300-500 km
TD	315	1290 *(1.6)*	117 *(3.7)*	633 *(2.5)*	541 *(1.0)*
TS	644	1802 *(2.2)*	202 *(6.4)*	741 *(2.9)*	859 *(1.7)*
C12	256	1665 *(2.1)*	80 *(2.5)*	642 *(2.6)*	943 *(1.9)*
C3+	243	1748 *(2.2)*	59 *(1.8)*	556 *(2.2)*	1134 *(2.2)*
RI	52	2105 *(2.7)*	174 *(5.5)*	642 *(2.6)*	1289 *(2.6)*

Table 10. Average 6-h flash rates for all categories and radial regions; with 6 h flash densities ((flashes km^{-2} 6 h^{-1}) $\times$ 10^{-3}) in parentheses.

Category	Sample Size	Storm Total 0-500 km	Inner Core 0-100 km	Outer Rainbands 100-300 km	Far Outer Bands 300-500 km
TD	168	2464 *(3.1)*	194 *(6.1)*	1282 *(5.1)*	988 *(1.9)*
TS	316	3594 *(4.6)*	362 *(11.5)*	1505 *(5.9)*	1727 *(3.4)*
C12	123	3375 *(4.3)*	181 *(5.7)*	1263 *(5.0)*	1931 *(3.8)*
C3+	117	3562 *(4.3)*	120 *(3.8)*	1176 *(4.7)*	2266 *(4.5)*
RI	15	4165 *(5.3)*	208 *(6.6)*	1180 *(4.7)*	2777 *(5.5)*

Table 11. Standard deviations of 6-h flash rates for all categories and radial regions.

Category	Sample Size	Storm Total 0-500 km	Inner Core 0-100 km	Outer Rainbands 100-300 km	Far Outer Bands 300-500 km
TD	168	*3140*	*479*	*2237*	*1252*
TS	316	*3879*	*692*	*2007*	*2469*
Category 1 & 2	123	*3946*	*579*	*2292*	*2144*
Category 3+	117	*2909*	*183*	*1433*	*2103*
RI	15	*2811*	*232*	*1058*	*2193*

Standard deviations of 6 h (Table 11) and 3 h flash rates (not shown) reveal that the IC region exhibits the smallest variability in flashes. The IC region contains greatest standard deviations during periods of TS intensity, with the C12 group showing the second greatest variability. Standard deviations in the IC of C3+ storms are ~250% smaller than the next smallest

category (C12). This indicates that IC flash rates in intense hurricanes typically change little from one observation period to the next. Flash rates in the IC of TDs, TSs, and C12 hurricanes are more variable. The OR region displays greatest variability during the TD stage, and smallest variability for C3+ storms and during RI. The FOB region exhibits small variability during TD intensity, but much greater variability during the other stages. Since the convective structure of C3+ hurricanes and TCs undergoing RI typically is well organized and has established regions of lightning (the eyewall and OR), there generally is less convective variability from one 6 or 3 h period to the next. Conversely, TDs, TSs, and weak hurricanes display bursts of convection in various regions of the storm that create large variability in the number and distribution of flashes from one period to the next. This is particularly true in the IC region. IC lightning during RI is more variable than in C3+ storms, indicating that lightning fluctuations are common during intensification but that C3+ hurricanes tend to have more constant IC flash activity.

3.2.2 Correlations between Lightning and Intensity Change

To determine whether CG lightning data have the potential to increase the skill of TC intensity forecasts, we computed correlations between flash rate and pressure change. Separate calculations were made using the 3 and 6 h data, and the lightning trends were analyzed for the period concurrent with the 3 and 6 h pressure interval and also for periods preceding (occurring before) and lagging (occurring after) the pressure change interval. Calculations were made for all categories and regions of the TCs (IC, OR, FOB, ST). As done previously, flash counts were removed when the storm center was over land. Scatter plots are used to visualize relations between flash rates and intensity changes, and coefficients of determination (R^2) quantify these relations. It should be noted that no statistical analyses were performed to determine statistical significance and that correlation values are assessed on a scale from 0 to 1 with 1 being the strongest possible relationship and 0 indicative of no relation. In order to carry out a more definite analysis, a t test would need to be completed to assess the statistical meaning of R^2 values. The discussion of R^2 in this study is sufficient to make general conclusions regarding relationships between CG lightning and TC intensity change.

Increasing flash rates usually are associated with increasing pressure falls (Table 12). However, the data in brackets denote the opposite relation, with greater flash counts favoring smaller pressure falls or even pressure rises. Many of the timeframes and regions exhibit near

zero R^2, indicating that lightning is poorly correlated with intensity fluctuations. This is especially true in the IC region where many categories and timeframes have R^2 ~0.00. Nonetheless, the IC region still contains the second greatest average R^2 (0.044) for all time periods due to several larger values in the lagging C3+ and RI categories. The ST region depicts the greatest average R^2 (0.047). The OR and FOB regions exhibit the smallest average R^2 (0.039 and 0.037, respectively). Averaged R^2 for all categories and timeframes reveals that greatest correlations occur when lightning either lags the 6 h pressure change (0.046) or when the two periods are concurrent (0.050). R^2 values when the lightning period precedes the pressure change period exhibit the weakest relationship (0.030). Although the small R^2 values when flash counts precede intensification suggest that 6 h CG flash counts are a poor predictor of future intensification, they will be examined further in the following paragraphs.

Table 12. Summary of R^2 between pressure change and lightning flash count (lagging, preceding, concurrent) for all 6 h categories and annular regions. Most values denote a negative correlation between lightning and pressure change, but bracketed values denote a positive correlation. Regional R^2 averages and average R^2 by time period in parentheses also are shown.

Storm Category	Timeframe	Storm Total Count (0-500 km)	Inner Core (0-100 km)	Outer Rainbands (100-300 km)	Far Outer Rainbands (300-500 km)
All Categories	*Concurrent*	0.03	~0.00	0.02	0.02
	Lagging	0.04	0.01	0.03	0.03
	Preceding	0.02	~0.00	0.02	0.02
Tropical Depressions	*Concurrent*	0.05	~0.00	0.03	0.06
	Lagging	0.04	0.01	0.03	0.01
	Preceding	0.04	0.02	0.07	0.03
Tropical Storms	*Concurrent*	0.03	~0.00	0.04	0.02
	Lagging	0.02	~0.00	0.02	0.01
	Preceding	0.01	0.01	0.01	0.01
Category 1 & 2 Hurricanes	*Concurrent*	0.04	~0.00	0.01	0.07
	Lagging	0.05	~0.00	0.03	0.06
	Preceding	0.04	~0.00	0.02	0.03
Category 3+ Hurricanes	*Concurrent*	0.03	0.02	0.02	0.01
	Lagging	0.03	**0.35**	0.04	~0.00
	Preceding	0.03	~0.00	0.04	0.01

Table 12 - continued…

Storm Category	Timeframe	Storm Total Count (0-500 km)	Inner Core (0-100 km)	Outer Rainbands (100-300 km)	Far Outer Rainbands (300-500 km)
Rapid Intensification Periods	*Concurrent*	**[0.26]**	0.05	**[0.21]**	**[0.19]**
	Lagging	~0.00	**0.27**	~0.00	[0.03]
	Preceding	[0.09]	[0.06]	[0.07]	[0.06]
Averages:	*All periods*	*0.047*	*0.044*	*0.039*	*0.037*
	Preceding(0.030)	*0.038*	*0.015*	*0.038*	*0.027*
	Lagging(0.046)	*0.030*	***0.107***	*0.025*	*0.023*
	Concurrent(0.050)	***0.073***	*0.012*	*0.055*	*0.061*
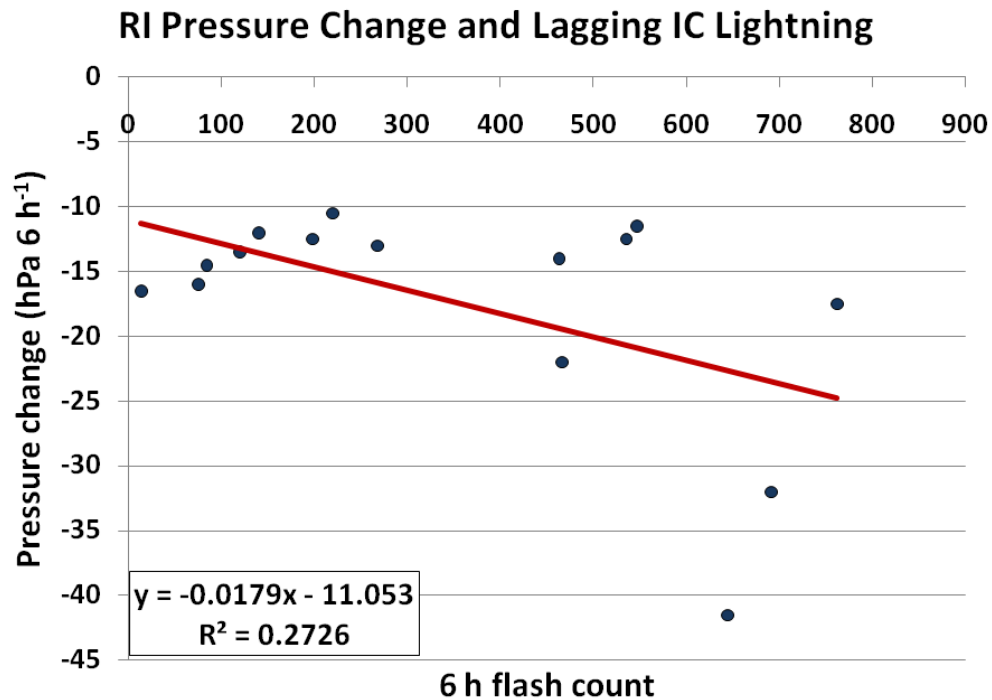
Figure 27. Scatter plot during periods of RI of 6 h flash count in the IC region that lag the pressure change period (hPa) . The linear best fit line and coefficient of determination (R^2) also are shown.

The greatest, but still small R^2 values (bold in Table 12) occur when IC lightning lags (occurs after) the intensification period in the C3+ and RI categories, and for the ST, OR, and FOB regions when flash counts are calculated concurrent with the RI periods. The C3+ and RI

periods are examined more closely using scatter diagrams (Figs. 27-30). The scatter diagram for RI periods with IC lightning lagging (occurring after) the pressure change period (Fig. 27) exhibits a negatively sloping best fit line which indicates that greater 6 h flash counts generally are associated with greater pressure falls. However, one should note that flash counts less than 300 flashes do not exhibit this tendency. Fig. 28 exhibits a similar relation for storms of C3+ intensity. Both figures suggest that increased lightning activity is more likely to follow intensification than precede it. Relatively large, but still small values of R^2 also occur in the RI category when flash rate and pressure change are concurrent (Figs. 29 and 30). However in these cases, large flash rates are associated with smaller pressure falls, an unexpected finding. The weaker intensity categories (not shown, TD, TS, and C12) exhibit virtually no relationship between lightning activity and preceding, concurrent, or lagging CG lightning in any region (Table 12).
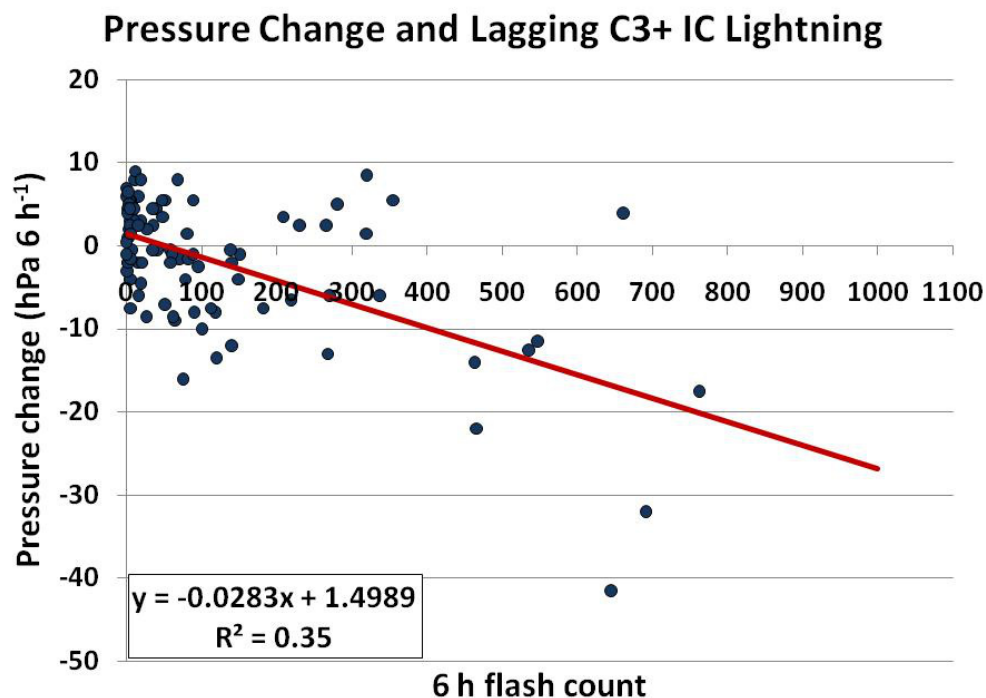
Figure 28. Scatter plot for C3+ hurricanes when the 6 h flash rate period lags the pressure change period (hPa). The linear best fit line and coefficient of determination (R^2) also are shown.
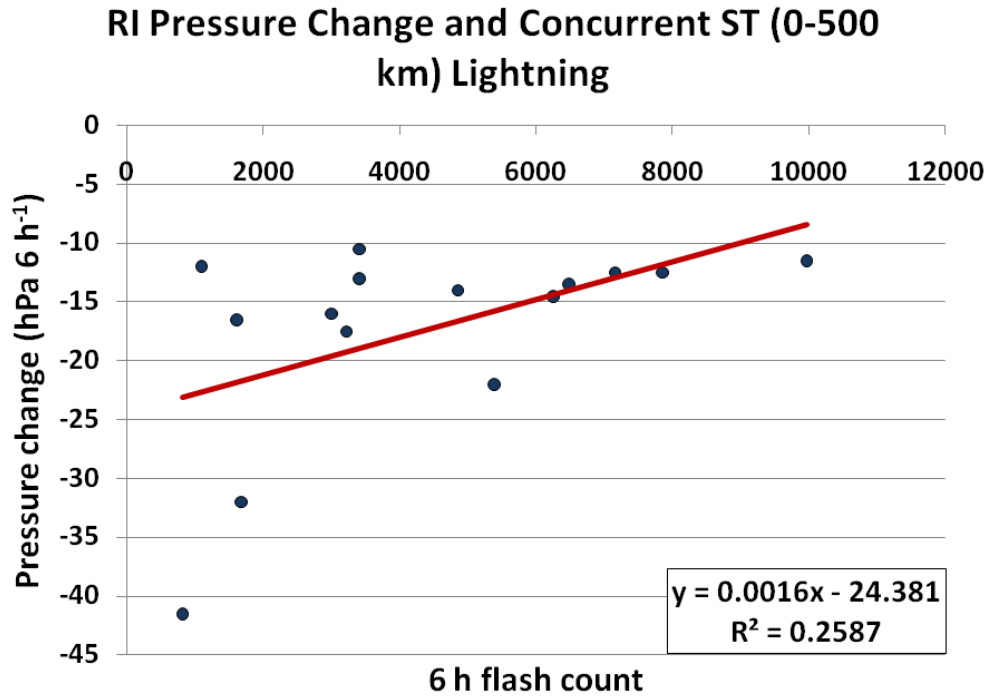
Figure 29. Scatter plot for the composite of all storm regions (ST) during periods of RI when the 6 h flash rate period is concurrent with the pressure change period (hPa). The linear best fit line and coefficient of determination (R^2) also are shown.

The discussion above utilized 6 h periods for calculating flash rates and pressure tendencies. We investigated whether 3 h periods would produce stronger relations. This approach is similar to Demetriades and Holle (2008) and Demetriades et al. (2010) who computed corrected 3 h cloud-to-ground IC flash rates for several TCs. The values of R^2 using 3 h periods (Table 13) generally are much smaller than those at 6 h (Table 12), with the greatest value being only 0.19 for C3+ storms when IC lightning lags the pressure change period. Most entries again show near-zero relationships. The IC region again exhibits the most periods when $R^2 \sim 0.00$. The FOBs contain the greatest average R^2 values (0.030), with the ST region being second largest (0.027). The IC and OR regions display the smallest average correlations at 0.018 and 0.012 respectively.
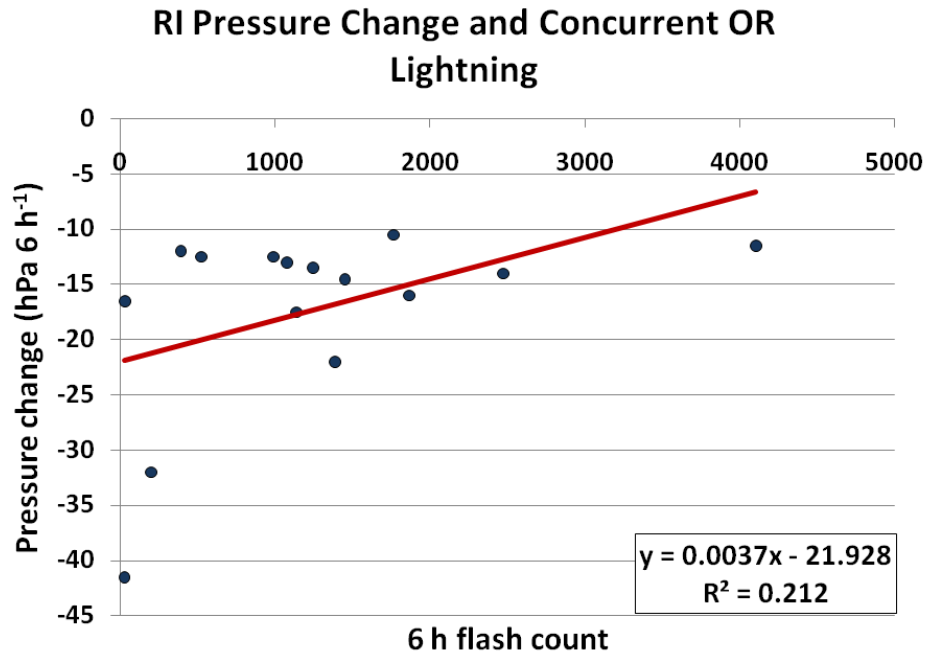
Figure 30. Scatter plot in the OR region during periods of RI with the 6 h flash rate period being concurrent with the pressure change period (hPa). The linear best fit line and coefficient of determination (R^2) also are shown.

Table 13. Summary of R^2 between pressure change and lightning flash count (lagging, preceding, concurrent) for all 3 h categories and annular regions. Most values denote a negative correlation between lightning and pressure change, but bracketed values denote a positive correlation. Regional R^2 averages and average R^2 by time period in parentheses also are shown.

Storm Category	Timeframe	Storm Total Count (0-500 km)	Inner Core (0-100 km)	Outer Rainbands (100-300 km)	Far Outer Rainbands (300-500 km)
All Categories	*Concurrent*	0.01	~0.00	~0.00	0.01
	Lagging	0.02	0.01	0.01	0.02
	Preceding	0.02	~0.00	0.01	0.02
Tropical Depressions	*Concurrent*	0.03	~0.00	0.01	0.04
	Lagging	0.02	0.01	0.01	0.01
	Preceding	0.04	~0.00	0.01	**0.10**
Tropical Storms	*Concurrent*	0.03	~0.00	0.03	0.02
	Lagging	0.04	0.01	0.02	0.02
	Preceding	0.02	~0.00	0.02	0.01

Table 13 - continued…

| Storm Category	Timeframe	Storm Total Count (0-500 km)	Inner Core (0-100 km)	Outer Rainbands (100-300 km)	Far Outer Rainbands (300-500 km)
Category 1 & 2 Hurricanes	*Concurrent*	0.03	~0.00	~0.00	0.06
	Lagging	0.03	0.01	0.01	0.03
	Preceding	0.02	~0.00	~0.00	0.05
Category 3+ Hurricanes	*Concurrent*	~0.00	0.04	0.01	~0.00
	Lagging	0.04	**0.19**	0.03	0.01
	Preceding	0.03	~0.00	0.01	0.03
Rapid Intensification Periods	*Concurrent*	[0.03]	~0.00	~0.00	[0.04]
	Lagging	[0.02]	0.04	~0.00	[0.04]
	Preceding	[0.06]	[0.02]	[0.04]	[0.03]
Averages:	*All periods*	*0.027*	*0.018*	*0.012*	*0.030*
	Preceding(0.022)	*0.032*	*0.003*	*0.015*	*0.040*
	Lagging(0.027)	*0.028*	*0.045*	*0.013*	*0.021*
	Concurrent(0.016)	*0.022*	*0.007*	*0.008*	*0.028*

Figure 31. Scatter plot for the IC region of C3+ hurricanes when the 3 h IC flash rate lags the pressure change period (hPa). The linear best fit line and coefficient of determination (R^2) also are shown.
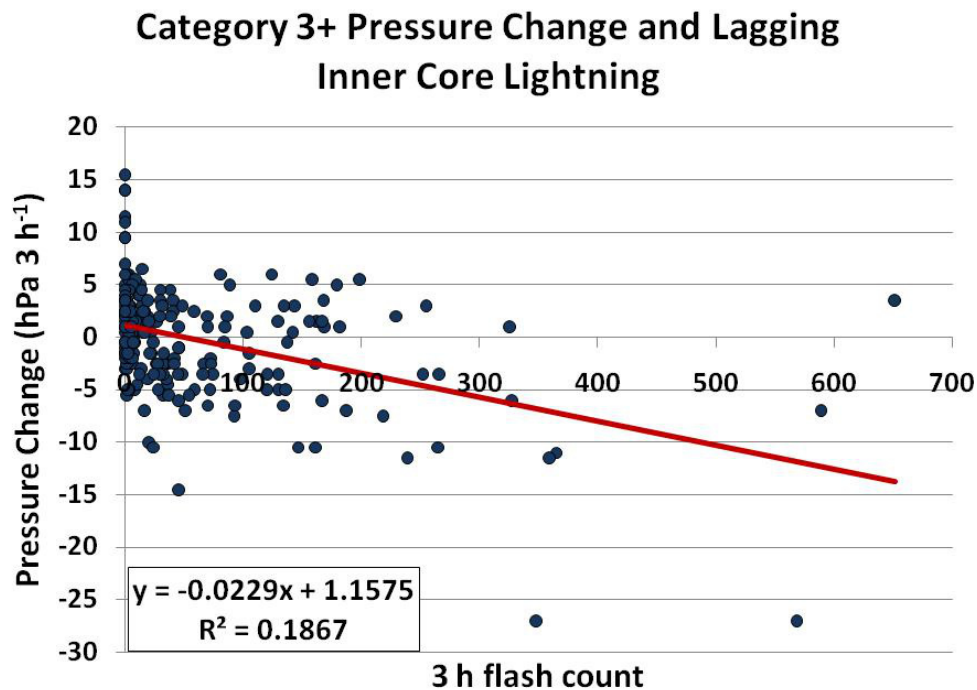
49

When assessing values by concurrent, lagging, and preceding timeframes, average R^2 when the lightning lags (0.027) or precedes (0.022) the pressure change exhibit the strongest relationships, with concurrent lightning showing the weakest (0.016) relation. The greatest 3 and 6 h values of R^2 (bold, Tables 12 and 13) are located in the IC region of C3+ hurricanes (Figs. 28, 31) when lightning lags the pressure change. R^2 for 3 h is 0.19, and for 6 h is 0.35. This indicates that the relationship over smaller timescales is worse than for longer periods. One should note that no 3 h values of R^2 during RI exceed 0.06, a disappointing finding.

In summary, values of R^2 for 3 and 6 h periods (Table 13) reveal virtually no lightning-pressure change relationship. The only exception is C3+ hurricanes that exhibit a weak relationship between lagging lightning and intensification (Figs. 28, 31). The application of a statistical t-test would allow for more definite conclusions regarding 3 and 6 h R^2 values. For this paper, a more empirical methodology allows us to deduce only generalized conclusions. We next present results over longer timescales to determine if stronger relationships can be found.

We calculated correlations (r) at 6 h intervals between ± 72 h (3 days) to determine if maximum storm-total (0-500 km) lightning activity precedes, lags, or is consistent with maximum sustained wind speed (maximum intensity) at these longer time scales. One should recall that Price et al. (2009) found that maximum lightning frequency preceded maximum sustained wind speed by approximately one day. They used total lightning data from the WWLLN and NHC best track 6 h positions and sustained wind speeds (kt). The Price et al. (2009) dataset consisted of lightning data for 58 category 4 and 5 hurricanes in a 10 degree by 10 degree latitude/longitude box centered on the NHC best track hurricane center. This box corresponds approximately to our 0-500 km (ST) radial region. Their time series of flash data and sustained winds were smoothed during the lifetime of the storm using a running average procedure. The smoothed lightning/wind speed curves then were temporally displayed and correlated at 6 h intervals for ±6 days, yielding a maximum correlation for each of the 58 hurricanes at a specific displacement time. In this study, we computed correlations for each of the 45 TCs at 6 h displacements totaling ±72 h between 6 h LLDN flash counts and 6 h sustained wind speeds (kt). To maintain data integrity, no smoothing was applied to the lightning or wind data. Fig. 32 shows a time series of correlations for hurricane Rita (2005) at each 6 h time-step between -72 h to +72 h. Rita is shown since it contained one of the greatest correlations between maximum lightning activity and maximum sustained winds (0.86). This occurred when wind

50

speeds were lagged 48 h from the lightning. Thus, Rita's maximum lightning activity precedes her maximum winds by 48 h. Rita's smallest correlation between lightning and maximum sustained wind speed (- 0.30) occurs at +36 h.
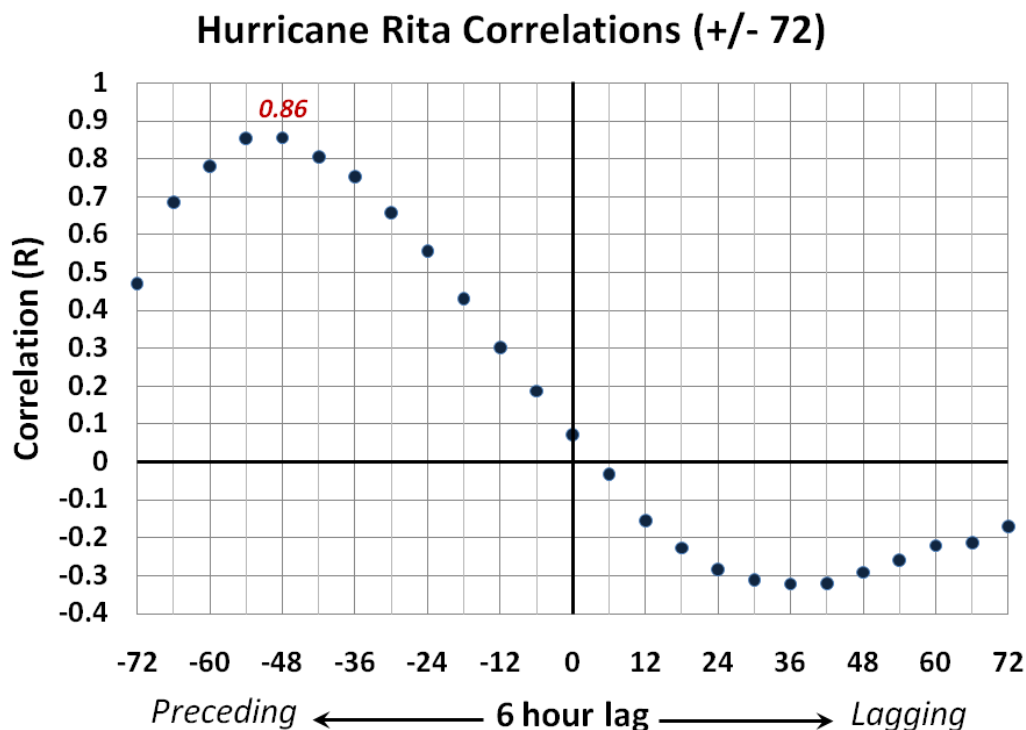
Figure 32. Plot of correlations (r) between lightning and wind speed (kt) (see text for details) for hurricane Rita (2005) over 6 h periods from -72 h to +72 h. Preceding (lagging) refers to maximum lightning occurring before (after) the maximum sustained wind speed (kt).

The time series of correlations for all 45 TCs were merged to seek a general relation between lightning and intensity (Fig. 33). One should note that some of the points in the figure overlap. While some storms exhibit large correlations at times, many points indicate a weak or even negative correlation. The greatest correlations generally are associated with lightning lagging the intensification by 18 to 24 h; however, some cases of lightning preceding intensification also display strong correlations. This analysis indicates that there is no general timing between greatest lightning activity and maximum sustained winds.
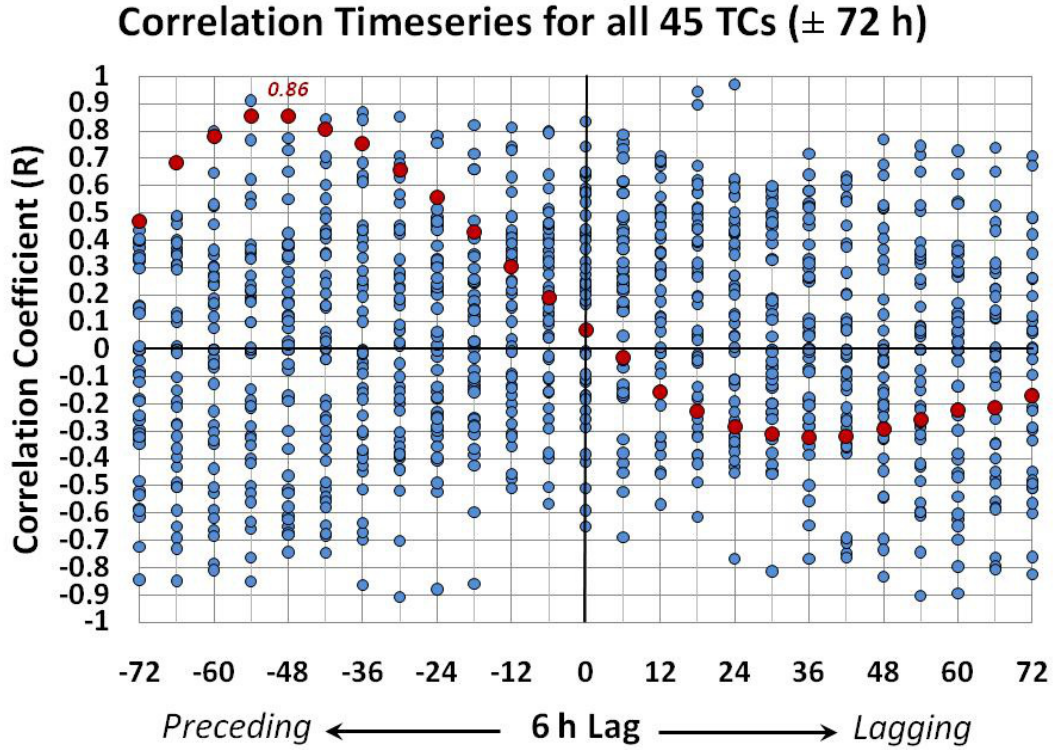
Figure 33. Plot of all 6 h correlations (r) between lightning and wind speed (kt) for all TCs from -72 h to +72 h. That is, all 45 versions of Fig. 32. Preceding (lagging) refers to maximum lightning occurring before (after) the maximum sustained wind speed (kt). The correlations for Hurricane Rita (2005) are plotted in red.

Following Price et al. (2009), maximum correlations from the time series for each of the 45 TCs were plotted (Fig. 34). The average maximum correlation of ~0.64 (R^2 ~ 0.41) (dashed red line), indicates that our sample at best displays only weak relationships between lightning frequency and wind speed. Despite several correlations exceeding 0.8, 14 of the 45 TCs exhibit maximum correlations less than 0.5, indicating little relation between lightning activity and maximum intensity (maximum sustained wind speed) for preceding, lagging, or concurrent lightning.
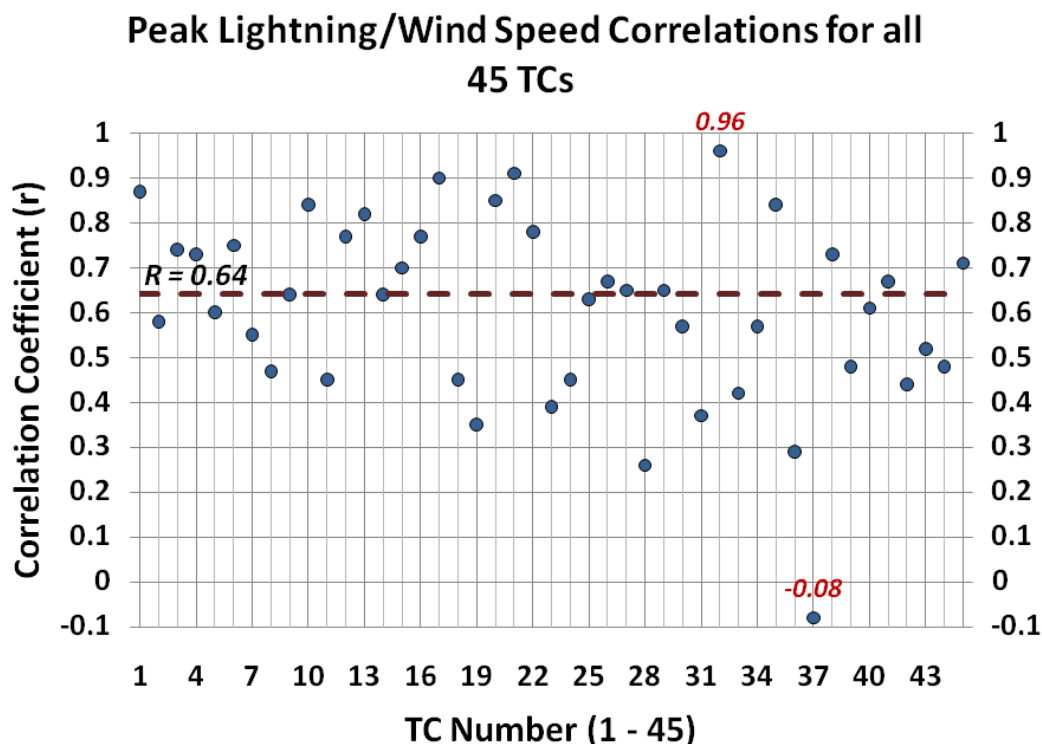
Figure 34. Plot of maximum 6 h correlations (r) between lightning and wind speed (kt) for all 45 TCs from -72 h to +72 h. The average of these maximum correlations (0.64) is indicated by the brown dashed line.

We next prepared a frequency plot (Fig. 35) similar to Price et al. (2009) by totaling those 6 h bins (-72 h to +72 h) that contained the maximum correlation for each storm. The peaks of 11% at -36 h and 9% at +18 h reveal that the strongest relations between maximum lightning and maximum sustained wind speed both precede and lag the 0 h (concurrent) observation. Thus, once again, there is no preferred timing between lightning and maximum sustained wind speed, echoing the results from Fig. 33. Since Price et al. (2009) only considered category 4 and 5 hurricanes; we then prepared a separate frequency diagram to display greatest correlation times for only our intense hurricanes (C3+) (Fig. 36). Values of 0 to 8% are evident over much of the time span, with no clear preference for any 6 h period. However, the most frequently occurring 6 h bin with
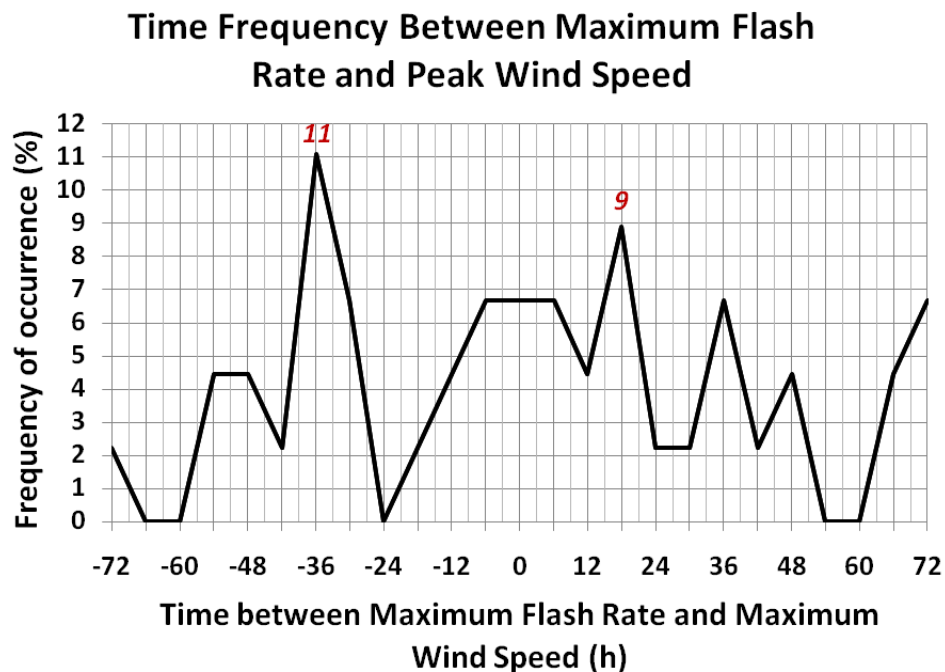
Figure 35. Frequency plot of maximum correlation (r) between lightning and wind speed (kt) for all 6 h bins (±72 h) (patterned after Price et al. 2009).
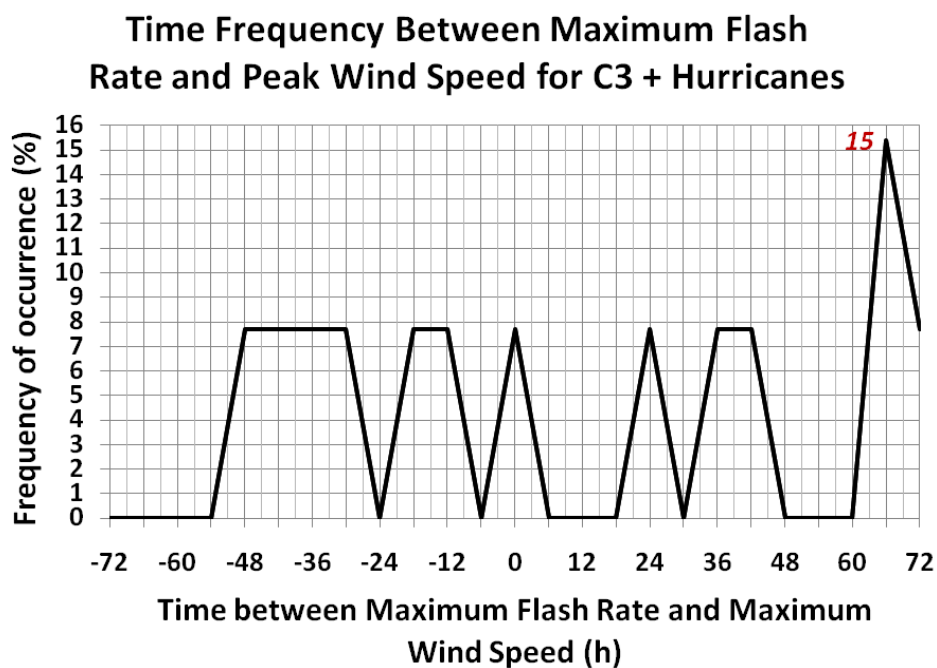
Figure 36. Frequency plot of maximum correlation (r) between lightning and wind speed (kt) for all C3+ storms using 6 h bins (±72 h) (patterned after Price et al. 2009).

maximum correlation is at +66 h (15% of bins). This result is inconsistent with Fig. 35 that indicated preferred times both preceding and lagging the concurrent (0 h) time. Thus, neither diagram produces results that agree with those of Price et al. (2009) who found that 70% of intense hurricanes had greatest lightning preceding the maximum sustained wind speed by approximately 24 h (1 day), with an average maximum correlation coefficient (r) of 0.82, ~33% larger than our sample. These conflicting results may result from the different lightning sources (WWLLN vs. LLDN), different storm samples, or slightly different methodologies in computing mean correlations between flash count and maximum sustained wind speed.

CHAPTER 4

SUMMARY AND CONCLUSIONS

Our understanding of TC's has improved greatly in recent years. TC track forecasts have become more accurate, but intensity forecasts have improved little (Fig. 1), and factors leading to intensity change continue to challenge the scientific community. The development of lightning detection networks has resulted in improved observations of convection in TCs over the open oceans. Of these networks, the LLDN provides the greatest detection efficiency of offshore CG lightning (Fig. 2). Various research has hypothesized that CG lightning may be useful in forecasting TC intensity.

Our study examined 45 Atlantic Basin TCs between the years 2004 and 2008 (Fig. 3, Table 1). Spatial distributions of composite CG flash density in north-relative, storm-relative, and shear-relative coordinates were presented (Figs. 8-22). Results showed that storm motion, forward speed, and wind shear influence the convective organization in the various TC categories (TD, TS, C12, and C3+). Lightning densities also were prepared during periods of intensification and weakening (SI, FI, RI, no change, and weakening) to establish relationships between intensity change and lightning density (Figs. 23-26).

North-relative flash densities (Fig. 8) revealed that weak TCs (TDs and TSs) generally are less organized, exhibiting weaker IC and OR signals than their stronger counterparts (C12 and C3+ hurricanes) (Fig. 8a, b). The hurricane intensity groups (Fig. 8c, d) contain more distinct distributions, with C3+ composites displaying eyewall (IC), OR, and FOB signals that are consistent with the idealized convective model of intense hurricanes (e.g., Molinari et al. 1999).

The storm-relative flash densities (Figs. 9-15) revealed that lightning activity and associated deep convection were preferred in the right front and rear TC quadrants as observed by Corbosiero and Molinari (2003). Greatest flash densities with respect to storm motion occurred in the IC region of hurricanes (Table 3) in association with the eyewall. Fast forward speed exhibited the greatest flash densities in the TD and TS storms (Figs. 10 and 11), while the C12 and C3+ groups displayed peak flash density during slow forward motion (Figs. 12-15). Periods

of FI and RI exhibited the greatest IC flash densities with the three weaker pressure change categories exhibiting similar IC flash densities (Table 7).

Assessing lightning distributions with respect to wind shear (Figs. 16-22) showed that lightning activity generally was most common in the downshear left and right quadrants in the IC and OR regions respectively, consistent with Corbosiero and Molinari (2002, 2003) and Abarca et al. (2010). Mechanisms producing this relation have been discussed by Frank and Ritchie (2001) and Reasor et al. (2004) who found that the downshear signal is related to convective resilience against shear-induced vortex tilting. This relation was most evident for TSs and hurricanes (Figs. 18-22), while TDs showed a preference for convection in the downshear right quadrant (Fig. 17), consistent with TDs being more susceptible to wind shear and vortex tilting. Moderate wind shear produced the greatest flash densities for TDs, TSs, and C12 hurricanes, with weak shear promoting greatest flash density in the C3+ hurricanes (Table 5). Strong wind shear resulted in the smallest flash densities (~0.014 flashes km^{-2} 6 h^{-1}) in all but the TS category due to a lack of deep convection and associated enhanced lightning activity. Wind shear during periods of RI and FI contained the greatest flash densities of all intensity change categories in the IC, with similar maximum density values for the three weaker categories and a stronger preference for the OR region (Figs. 25 and 26, Table 8).

Calculations of average categorical flash rates and densities were produced to compare flash frequency for the various storm categories and regions. Coefficients of determination (R^2) were computed between periods of pressure change and lagging, preceding, and concurrent lightning periods to explore relationships between CG flash activity and intensity change. Longer term correlations (r) also were calculated following Price et al. (2009) to determine whether peak flash activity was offset from maximum sustained wind speed (i.e., maximum intensity).

Average flash rates and densities varied greatly by storm category, with TSs showing the greatest average 3 and 6 h flash rates in all regions but the FOB, consistent with Demetriades and Holle (2008) and Demetriades et al. (2010) who showed that 3 h IC flash rates were greatest for TSs (Tables 9 and 10). Hurricanes (C12, C3+) exhibited less IC flash activity than the weaker intensity categories, with the most intense hurricanes (C3+) containing the smallest IC and OR flash rates. Flash rates in the FOB region increased with increasing intensity, with TDs having the smallest average flash rates and intense hurricanes having the greatest. In terms of ST lightning, TSs produce the greatest flash rates followed by the C3+ and C12 hurricane groups. 3

and 6 h flash rates during periods of RI contained the greatest average flash rates in all regions except the OR. The small flash rates in the more intense hurricanes stems from the preference for lightning and convection to have a strong radial organization. Due to the development of the inner rainband in strong TCs (Molinari et al. 1999), lightning is confined to the IC and OR regions where deep convection develops. Weaker systems (TDs and TSs) contain infrequent bursts of convection which produce disorganized regions of lightning activity throughout the 500 km radius. Although the greatest number of flashes occurred in the OR and FOB regions, lightning activity with respect to area (flash density) was maximized in the IC region associated with the eyewall, especially in hurricanes (Tables 9 and 10).

Our statistical results (Tables 12 and 13) indicate that lightning generally is poorly correlated with pressure change. Greatest correlations occur during periods of C3+ intensity (R^2 = 0.35) and during RI (R^2 = 0.27) when IC lightning lags (comes after) the pressure falls. Both values indicate a very weak relationship. This suggests that CG lightning is a poor indicator of impending intensity change. While there certainly are cases of storms in which lightning precedes intensification (e.g., Hurricanes Katrina (2005) and Rita (2005) from Squires and Businger 2008), our composite results from 45 storms of various intensity categories and in various regions of the TCs display no consistent time-dependent relationships.

Applying the methods of Price et al. (2009) to our sample showed virtually no time-dependent relationship between peak lightning and maximum sustained wind speed (Figs. 32-36). Average maximum correlation coefficients between maximum sustained wind speed and lightning were weak (r = ~0.64) (Fig. 34). Considering the entire storm sample, maximum lightning has no clear time preference with respect to maximum sustained wind speed, with at most 11% of the maximum r values occurring 36 h before the 0 h (concurrent) bin (Fig. 35). When only intense hurricanes were considered, even weaker relations were found, with a maximum frequency of 15% when lightning lags maximum sustained wind speed by more than 60 h (Fig. 36). No other 6 h bins produce maximum correlations greater than 8% of the time. Thus, there do not appear to be meaningful longer term temporal relationships between CG lightning and maximum sustained wind speed in C3+ hurricanes.

Our results show that CG lightning should be regarded as a poor indicator of TC intensity change and that its use alone will not provide the increased skill in TC intensity forecasting that is so desperately needed. The development of improved geostationary satellite platforms capable

of detecting total lightning, such as GOES-R, along with new data assimilation and modeling techniques hopefully will take better advantage of lightning data, leading to improved TC intensity forecasts.

REFERENCES

Aberson, S. D., 2002: Two years of operational hurricane synoptic surveillance. *Wea. Forecasting*, **17**, 1101-1110.

Aberson, S. D., 2003: Targeted observations to improve operational tropical cyclone track forecast guidance. *Mon. Wea. Rev.*, **131**, 1613-1628.

Aberson, S. D., 2010: 10 years of hurricane synoptic surveillance (1997-2006). *Mon. Wea. Rev.*, **138**, 1536-1549.

Abarca, S. F., K. L. Corbosiero, and D. Vollaro, 2010: The world wide lightning location network and convective activity in tropical cyclones. *Mon. Wea. Rev.*, in press.

Black, R. A., and J. Hallett, 1986: Observations of the distribution of ice in hurricanes. *J. Atmos. Sci.*, **43**, 802-822.

Black, R. A. and J. Hallett, 1999: Electrification of the hurricane. *J. Atmos. Sci.,* **56**, 2004-2028.

Boccippio, D. J., S. J. Goodman, and S. Heckman, 2000: Regional differences in tropical lightning distributions. *J. Appl. Meteor.*, **39**, 2231-2248

Braun, S. A., M. T. Montgomery, and Z. Pu, 2006: High-resolution simulation of Hurricane Bonnie (1998). Part I: The organization of eyewall vertical motion. *J. Atmos. Sci.*, **63**, 19-42.

Braun, S. A., and L. Wu, 2007: A numerical study of Hurricane Erin (2001). Part II: Shear and the organization of eyewall vertical motion. *Mon. Wea. Rev.,* **135**, 1179-1194.

Cecil, D. J. and E. J. Zipser, 1999: Relationships between tropical cyclone intensity and satellite-based indicators of inner core convetion: 85-GHz ice-scattering signature and lightning. *Mon. Wea. Rev.,* **127**, 103-123.

Cecil, D. J., E. J. Zipser and S. W. Nesbitt, 2002: Reflectivity, ice scattering, and lightning characteristics of hurricane eyewalls and rainbands. Part I: quantitative description. *Mon. Wea. Rev.,* **130**, 769-784.

Cecil, D. J., E. J. Zipser and S. W. Nesbitt, 2002: Reflectivity, ice scattering, and lightning characteristics of hurricane eyewalls and rainbands. Part II: Intercomparison of observations. *Mon. Wea. Rev.,* **130**, 785-801.

Corbosiero, K.L., and J. Molinari, 2002: The effects of vertical wind shear on the distribution of convection in tropical cyclones. *Mon. Wea. Rev.*, **130**, 2110-2123.

Corbosiero, K.L., and J. Molinari, 2003: The relationship between storm motion, vertical wind shear, and convective asymmetries in tropical cyclones. *J. Atmos. Sci.*, **60**, 366-376.

Cramer, J. A., and K. L. Cummins, 1999: Long-range and transoceanic lightning detection. *Proc. 11th Int. Conf. on Atmospheric Electricity,* Guntersville, AL, NASA/CP 1999-209261, 250–253.

Cummins, K. L., M. J. Murphy, E. A. Bardo, W. L. Hiscox, R. B. Pyle, and A. E. Pifer, 1998: A combined TOA/MDF technology upgrade of the U.S. national lightning detection network. *J. Geophys. Res.*, **103**, 9035-9044.

Cummins, K. L., J. A. Cramer, C. Biagi, E. P. Krider, J. Jerauld, M. Uman, and V. Rakov, 2006: The U.S. national lightning detection network: Post-upgrade status. Preprints, *Second Conf. on Meteorological Applications of Lightning Data*, Atlanta, GA, Amer. Meteor. Soc., 6.1.

Cummins, K. L., and M. J. Murphy, 2009: An overview of lightning locating systems: History, techniques, and data uses, with an in depth look at the U.S. NLDN. IEEE Trans. Electromag. Compat., 51 (3), 499–518.

DeMaria, M. and J. Kaplan, 1999: An updated statistical hurricane intensity prediction scheme (SHIPS) for the Atlantic and eastern north Pacific basins. *Wea. Forecasting*, **14**, 326-337.

DeMaria, M., M. Mainelli, L. K. Shay, J. A. Knaff, and J. Kaplan, 2005: Further improvements to the statistical hurricane intensity prediction scheme (SHIPS). *Wea. Forecasting*, **20**, 531-543.

Demetriades, N. W. S., and R. L. Holle, 2005: Long-range lightning applications for hurricane intensity. Preprints, *First Conf. on Meteorological Applications of Lightning Data*, San Diego, CA, Amer. Meteor. Soc., P2.8.

Demetriades, N. W. S., J. Molinari, and R. L. Holle, 2006: Long range lightning nowcasting applications for tropical cyclones. Preprints, *Second Conf. on Meteorological Applications of Lightning Data*, Atlanta, GA, Amer. Meteor. Soc., P2.15.

Demetriades, N. W. S. and R. L. Holle, 2008: Analysis of inner core lightning rates in 2004-2007 Atlantic and east pacific tropical cyclones using Vaisala's long range lightning detection network. Preprints, *International Lightning Meteorology Conference*, April 24-25 Tucson, AZ, Vaisala, 9 pp.

Demetriades, N. W. S., R. L. Holle, S. Businger, and R. D. Knabb, 2010: Eyewall lightning outbreaks and tropical cyclone intensity change. *29th Conference on Hurricanes and Tropical Meteorology*, May 9-14, Tucson, AZ, [Available online at *ams.confex.com/ams/29Hurricanes/techprogram/paper_168543.htm*].

Eastin, M. D., W. M. Gray, and P. G. Black, 2005: Buoyancy of convective vertical motions in the inner core of intense hurricanes. Part II: Case studies. *Mon. Wea. Rev.*, **133**, 209-227.

Fierro, A., L. Leslie, E. Mansell, J. Straka, D. MacGorman, and C. Ziegler, 2007: A high-resolution simulation of microphysics and electrification in an idealized hurricane-like vortex., *Meteor. Atmos. Phys.*, **98**, 13-33.

Frank, W. M. and E. A. Ritchie, 2001: Effects of vertical wind shear on the intensity and structure of numerically simulated hurricanes. *Mon. Wea. Rev.*, **129**, 2249-2269.

Goerss, J. S., C. R. Sampson, and J. M. Gross, 2004: A history of western north Pacific tropical cyclone track forecast skill. *Wea. Forecasting*, **19**, 633-638.

Hanley, D., J. Molinari, and D. Keyser, 2001: A composite study of the interactions between tropical cyclones and upper-tropospheric troughs. *Mon. Wea. Rev.*, **129**, 2570-2584.

Houze, R. A. and Coauthors, 2006: The hurricane rainband and intensity change experiment: Observations and modeling of hurricanes Katrina, Ophelia, and Rita. *Bull. Amer. Meteor. Soc.*, **87**, 1503-1521.

Idone, V. P., D. A. Davis, P. K. Moore, Y. Wang, R. W. Henderson, M. Rise, and P. F. Jamason, 1998a: Performance evaluation of the U.S. National Lightning Detection Network in eastern New York. Part I: Detection efficiency. *J. Geophys. Res.,* **103 (D8),** 9045–9055.

Idone, V. P., D. A. Davis, P. K. Moore, Y. Wang, R. W. Henderson, M. Rise, and P. F. Jamason, 1998b: Performance evaluation of the U.S. National Lightning Detection Network in eastern New York. Part II: Location accuracy. *J. Geophys. Res.,* **103 (D8),** 9057–9069.

Igau, R. C., M. A. LeMone, and D. Wei, 1999: Updraft and downdraft cores in TOGA COARE: Why so many buoyant downdraft cores? *J. Atmos. Sci.*, **56**, 2232-2245.

Jacobson, A. R., R. Holzworth, J. Harlin, R. Dowden and E. Lay, 2006: Performance assessment of the World Wide Lightning Location Network (WWLLN), Using the Los Alamos sferics array (LASA) as ground truth. *J. Atmos. Oceanic Technol.*, **23,** 1082-1092.

Jorgensen, D. P., 1984: Mesoscale and convective-scale characteristics of mature hurricanes Part 1: General observations by research aircraft. *J. Atmos. Sci.*, **41**, 1268-1286.

Jorgensen, D. P., and M. A. LeMone, 1989: Vertical velocity characteristics of oceanic convection. *J. Atmos. Sci.*, **46**, 621-640.

Khain, A., N. Cohen, B. Lynn, and A. Pokrovsky, 2008: Possible aerosol effects on lightning activity and structure of hurricanes. *J. Atmos. Sci.*, **65**, 3652-3677.

Khain, A., B. Lynn, and J. Dudhia, 2010: Aerosol effects on intensity of landfalling hurricanes as seen from simulations with the WRF model with spectral bin microphysics. *J. Atmos. Sci.*, **67**, 365-384.

Krishnamurti, T. N., S. Pattnaik, L. Stefanova, T. S. V. Vijaya Kumar, B. P. Mackey, A. J. O'Shay, and R. J. Pasch, 2005: The hurricane intensity issue. *Mon. Wea. Rev.*, **133**, 1886-1912.

Lascody, R. L., 1993: A different look at Hurricane Andrew – Lightning around the eyewall. *Natl. Wea. Dig.*, **17**, 39-40.

Leary, L. A., and E. A. Ritchie, 2009: Lightning flash rates as an indicator of tropical cyclone genesis in the eastern North Pacific. *Mon. Wea. Rev*., **137**, 3456-3470.

Leppert II, K.D., and W.A. Petersen, 2010: Electrically active hot towers in African easterly waves prior to tropical cyclogenesis. *Mon. Wea. Rev.*, **138**, 663-687.

Lucas, C., E. J. Zipser, and M. A. LeMone, 1994: Vertical velocity in oceanic convection off tropical Australia. *J. Atmos. Sci.*, **51**, 3183-3193.

Lyons, W. A., M. G. Venne, P. G. Black, and R. C. Gentry, 1989: Hurricane lightning. A new tool for tropical storm forecasting? Preprints. *18th Conf. on Hurricanes and Tropical Meteorology*, San Diego, CA, Amer. Meteor. Soc., 113-114.

Lyons, W. A. and C. S. Keen, 1994: Observations of lightning in convective supercells within tropical storms and hurricanes. *Mon. Wea. Rev.*, **122**, 1897-1916.

Molinari, J. and D. Vollaro, 1989: External influences on hurricane intensity. Part I: Outflow layer eddy angular momentum fluxes. *J. Atmos. Sci.*, **46**, 1093-1105.

Molinari, J., P. K. Moore, V. P. Idone, R. W. Henderson, and A.B. Saljoughey. 1994: Cloud-to-ground lightning in Hurricane Andrew. *J. Geophys. Res.*, **99**, 16 665-16 676.

Molinari, J., P. K. Moore, and V. P. Idone, 1999: Convective structure of hurricanes as revealed by lightning locations. *Mon. Wea. Rev.,* **127**, 520-534.

Molinari, J., D. Vollaro, and K.L. Corbosiero, 2004: Tropical cyclone formation in a sheared environment: A case study. *J. Atmos. Sci.*, **61**, 2493-2509.

Molinari, J. and D. Vollaro, 2010: Rapid intensification of a sheared tropical storm. *Mon. Wea. Rev.*, **138**, 3869-3885.

Murphy, M. J., and R. L. Holle, 2005: Where is the real cloud-to-ground lightning maximum in North America? *Wea. Forecasting*, **20**, 125-133.

Orville, R. E. and A. C. Silver, 1997: Lightning ground flash density in the contiguous United States: 1992-95, *Mon. Wea. Rev.*, **125**, 631-638.

Orville, R. E., and G. R. Huffines, 2001: Cloud-to-ground lightning in the United States: NLDN results in the first decade, 1989-98. *Mon. Wea. Rev.*, **129**, 1179-1193.

Orville, R. E., G. R. Huffines, W. R. Burrows, R. L. Holle, and K. L. Cummins, 2002: The north American lightning detection network (NALDN)- First results: 1998-2000. *Mon. Wea. Rev.*, **130**, 2098-2109.

Orville, R. E., 2008: Development of the National Lightning Detection Network. *Bull. Amer. Meteor. Soc.*, **89**, 180-190.

Price, C., M. Asfur, and Y. Yair, 2009: Maximum hurricane intensity preceded by increase in lightning frequency. *Nature Geosci.*, **2**, 329-332, doi:10.1038.NGEO477.

Pessi, A. T., S. Businger, K. L. Cummins, N. W. S. Demetriades, M. Murphy, and B. Pifer, 2009: Development of a long-range lightning detection network for the Pacific: construction, calibration, and performance. *J. Atmos. Oceanic Technol.*, **26**, 145-166.

Reasor, P. D., M. T. Montgomery, and L. D. Grasso, 2004: A new look at the problem of tropical cyclones in vertical shear flow: Vortex resiliency. *J. Atmos. Sci.,* **61,** pp. 3-22.

Rodger, C. J., J. B. Brundell, and R. L. Dowden, 2005: Location accuracy of VLF World Wide Lightning Location (WWLL) network: Post-algorithm upgrade. *Ann. Geophys.*, **23**, 277-290.

Rodger, C. J., S. Werner, J. B. Brundell, E. H. Lay, N. R. Thomson, R. H. Holzworth, and R. L. Dowden, 2006: Detection efficiency of the VLF World-Wide Lightning Location Network (WWLLN): Initial case study. *Ann. Geophys.*, **24**, 3197–3214.

Samsury, C.E., and R.E. Orville, 1994: Cloud-to-ground lightning in tropical cyclones: A study of Hurricanes Hugo (1989) and Jerry (1989). *Mon. Wea. Rev.*, **122**, 1887-1896.

Squires, K. and S. Businger, 2008: The morphology of eyewall lightning outbreaks in two category 5 hurricanes. *Mon. Wea. Rev.*, **136**, 1706-1726.

Sun, D., K. M. Lau, and M. Kafatos, 2008: Contrasting the 2007 and 2005 hurricane seasons: Evidence of possible impacts of Saharan dry air and dust on tropical cyclone activity in the Atlantic basin. *Geophys. Res. Lett.*, **35**, L15405, doi:10.1029/2008GL034529.

Toracinta, E. R. and E. J. Zipser, 2001: Lightning and SSM/I-ice-scattering mesoscale convective systems in the global tropics. *J. Appl. Meteor.*, **40**, 983-1002.

Toracinta, E. R., D. J. Cecil, E. J. Zipser, and S. W. Nesbitt, 2002: Radar, passive microwave, and lightning characteristics of precipitating systems in the tropics. *Mon. Wea. Rev.*, **130**, 802-824.

Willis, P. T., and F. D. Marks Jr., 1987: Convective scale transports in a mature hurricane. *Preprints. 17th Conf. on Hurricanes and Tropical Meteorology,* Miami, Amer. Meteor. Soc., 343-346.

Wingo, M. T. and D. J. Cecil, 2008: Effects of vertical wind shear on tropical cyclone precipitation. *Mon. Wea. Rev.*, **138**, 645-662.

Zipser, E. J., and M. A. LeMone, 1980: Cumulonimbus vertical velocity events in GATE II Part II. Synthesis and model core structure. *J. Atmos. Sci.*, **37**, 2458-2469.

BIOGRAPHICAL SKETCH

Marcus Austin was born in Miami, Oklahoma in the summer of 1984. He moved to Gainesville, Florida when he was three and developed an interest in severe weather at an early age. The main events which drove his passion for weather were the March 1993 "Super storm" and the Oklahoma tornado outbreak of May 3, 1999. Because the University of Florida lacked a meteorology program, Marcus enrolled in meteorology at the Florida State University. He obtained his B.S. degree in meteorology from Florida State University in spring semester 2008. Marcus enrolled in graduate school at Florida State University in the fall of 2008. Under the guidance of Dr. Henry Fuelberg, he sought to complete his M.S. in meteorology studying lightning in tropical cyclones.

Marcus' major research interests include lightning and convective processes in tropical cyclones leading to intensity change. Marcus also enjoys observing and documenting mesoscale severe weather including supercell thunderstorms and tornadoes. Over the years, Marcus has learned a great deal about meteorological phenomena and has garnered a healthy respect for their power and beauty.